We are IntechOpen, the world's leading publisher of Open Access books Built by scientists, for scientists

4,800
Open access books available

122,000
International authors and editors

135M
Downloads

Our authors are among the

154
Countries delivered to

TOP 1%
most cited scientists

12.2%
Contributors from top 500 universities

CLARIVATE ANALYTICS BOOK CITATION INDEX INDEXED

WEB OF SCIENCE™

Selection of our books indexed in the Book Citation Index in Web of Science™ Core Collection (BKCI)

Interested in publishing with us?
Contact book.department@intechopen.com

Numbers displayed above are based on latest data collected.
For more information visit www.intechopen.com

3

Coherent Laser Manipulation of Ultracold Molecules

Elena Kuznetsova[1,2], Robin Côté[1] and S. F. Yelin[1,2]
[1]*Department of Physics, University of Connecticut, Storrs, Connecticut*
[2]*ITAMP, Harvard-Smithsonian Center for Astrophysics, Cambridge, Massachusetts*
United States

1. Introduction

The realization of rovibrationally stable dense samples of ultracold diatomic molecules remains one of the main stepping stones to achieve the next slate of major goals in the field of atomic and molecular physics. Though obtaining diatomic alkali molecules was seen as a logical next step following the optical cooling of atoms, many of the possible applications currently under investigation extend beyond atomic and molecular physics. For example, spectroscopy of ultracold molecules can help in testing extensions of the Standard Model via the search for a permanent electric dipole moment of the electron (1; 2), or the energy difference between enantiomers of chiral molecules (3). Various molecular transitions can be utilized to track the time dependence of fundamental constants, including the fine structure constant and the proton to electron mass ratio (4). They also open the way for cold and ultracold chemistry, where the interacting species and products are in a coherent quantum superposition state (5) and reactions can happen via quantum tunneling. Dipolar ultracold quantum gases promise to show a plethora of new phenomena due to anisotropic long-range dipole-dipole interactions (6). Dipolar molecules in optical lattices can be employed as a quantum simulator of condensed matter systems, and they are predicted to demonstrate new quantum phases such as a dipolar crystal, supersolid, checkerboard and collapse phases (7; 8). Ultracold polar molecules also represent an attractive platform for quantum computation (9). They offer a variety of long-lived states for qubit encoding, including rotational, spin and hyperfine (if electronic and nuclear spins are non-zero), Λ and Ω-doublet states (10) and scalability to a large number of qubits. Polar molecules can be easily controlled by DC electric and magnetic fields, as well as by microwave and optical fields, allowing the design of various traps (11; 12). The main appeal of polar molecules for quantum information processing, however, comes from their permanent electric dipole moment, permitting them to interact via a long-range dipole-dipole interaction. The dipole-dipole interaction offers a tool to construct two-qubit gates, required for universal quantum computation (9; 13).

Ultracold molecules in their ground vibrational state $v = 0$ (and even in specific rotational, hyperfine or Zeeman states) are required for many of these applications since they have a large permanent electric dipole moment and are stable with respect to collisions and spontaneous emission. Currently translationally ultracold (100 nK - 1 mK) molecules are produced by magneto- (14) and photo-association (15) techniques. In a typical photoassociation scheme,

a pair of colliding atoms is photoassociated into a bound electronically excited molecular state that spontaneously decays, forming molecules in the electronic ground state. In magnetoassociation, a magnetic field is adiabatically swept across a Feshbach resonance, converting two atoms from a scattering state into a bound molecular state. These techniques have most successfully been applied to form alkali dimers from ultracold alkali metal atoms (14–16). In both techniques the molecules are translationally cold, but vibrationally hot, since they are formed in high vibrational states near a dissociation limit of the electronic ground state. Therefore, once created, molecules have to be rapidly transfered to the ground rovibrational state.

Basically all successfull methods for cooling vibrational (and rotational) degrees of freedom require refined laser pulse techniques from simple STIRAP pulses to optical control. In the recent past, several methods have been proposed to reach this goal: they can be divided into non-coherent and coherent techniques. Non-coherent methods include the pump-dump technique and radiative vibrational cascade. In the pump-dump technique a pump pulse transfers population from an initial state to some intermediate vibrational level of an electronically excited state, followed by a dump pulse which brings the population from the intermediate to the ground vibrational level (17). Ultracold molecules in the ground vibrational state have been produced using this technique in a photoassociation experiment (16) with a 6% efficiency. The pump-dump technique requires pulses shorter than the excited state lifetime (large intensity is therefore needed to achieve reasonable transfer efficiency). The transfer efficiency is low, unless pulses of specific area (e.g. π pulses) are used. To increase the transfer efficiency and avoid losses due to spontaneous emission from the excited electronic state, a sequence of alternating short pump and dump pulses can be applied, each transferring a small fraction of the population to the target state (18). Pulses in this case can be weak, since each has to transfer only a small fraction of the population. Additional spectral shaping of the pulses can provide population transfer to a desirable target state, where population is coherently accumulated. In this case molecules formed in the ground vibrational state have to be removed from the interaction volume to avoid excitation by subsequent pulses, leading to increase in the duration of the transfer process. In the second non-coherent method molecules in the ground electronic state are allowed to radiatively decay from the initial high vibrational level reaching the ground $v = 0$ state after several decay steps (19). In this case many intermediate vibrational states are populated which would result in loss of molecules from a trap due to vibrationally inelastic collisions with background atoms and formed molecules. Another incoherent technique, named molecular optical pumping (20), allows to transfer molecules from high vibrational states to the ground state using a shaped laser pulse. Molecules are excited to vibrational levels of higher-energy electronic states and spontaneously decay back to the ground one. The excited state vibrational levels are chosen to have a good Franck-Condon factors with the $v = 0$ vibrational level in the ground electronic state. The laser pulse is spectrally shaped so that all frequencies allowing molecules to be excited back from the $v = 0$ state are removed, and a significant fraction of molecules accumulates in the ground vibrational state after a few excitation- spontaneous emission cycles.

The major coherent methods are adiabatic passage and coherent control techniques. The latter one utilizes spectrally shaped broadband optical pulses to transfer the molecules from an initial to the ground vibrational state with high efficiency (21). Stimulated Raman Adiabatic Passage (STIRAP) (22) has recently attracted significant interest as an efficient way to produce

deeply bound molecules, starting from Feshbach molecules (23; 24). It allows to realize high transfer efficiency and preserve the high phase-space density of an initial atomic gas. In STIRAP, the laser pulses, coupling an initial and a final state to an intermediate excited state, are applied in a counter-intuitive sequence where a pump pulse is preceeded by a Stokes pulse. During the transfer, the system stays in a “dark" state, *i.e.*, a coherent superposition of initial and final states, preventing any losses that would otherwise occur from the excited state. By adiabatically changing amplitudes of the laser pulses, the “dark" state evolves from the initial to the final state, resulting in nearly 100% transfer efficiency. A STIRAP transfer from a Feshbach to a next lower vibrational state of a ground electronic potential has been demonstrated in $^{87}Rb_2$ molecules held in an optical lattice to avoid inelastic collisions (25). Recently, heteronuclear $^{40}K^{87}Rb$ molecules have been transferred from a Feshbach to a deeply bound ($>$ 10 GHz binding energy) vibrational state using STIRAP (26). Prospects of STIRAP-based photoassociation of a thermal ensemble of ^{85}Rb atoms have recently been analyzed theoretically in (27). Finally, in breakthrough experiments at JILA and Innsbruck ultracold weakly bound KRb (23) and Cs_2 (24) Feshbach molecules have been successfully brought to their ground rovibrational state via two- and multi-photon STIRAP, respectively.
In principle, STIRAP allows lossless transfer of the population from an initial to the target state with 100 % efficiency. The main difficulty with a two-pulse STIRAP in molecules is to find an intermediate vibrational state of the excited electronic potential which has a good Franck-Condon overlap with both highly delocalized initial high vibrational state and a tightly localized ground vibrational state (28). It is particularly difficult for homonuclear atoms having the ground electronic potential scaling as $1/R^6$ and the first excited potentials as $1/R^3$ with interatomic distance R, resulting in a non-favorable potential curves' overlap. It is less an issue for heteronuclear molecules having both potentials falling off with distance according to the $1/R^6$ law, making the overlap better and enabling a one-step STIRAP (23). It was therefore proposed in (29) to transfer population in several steps down the ladder of vibrational states using a sequence of stimulated optical Raman transitions. In this case the initial and final vibrational levels of each step do not differ significantly, and it is easier to find a suitable intermediate vibrational level in the excited electronic state. In this step-wise approach, however, the population is transfered through a number of vibrational levels in the ground electronic state subject to vibrational relaxation due to inelastic collisions with a background atom or another molecule. The released kinetic energy greatly exceeds the trap depth resulting in loss of both molecules and atoms from the trap. The step-wise transfer therefore has to be faster than the vibrational relaxation time. In the next section we describe a multistate chainwise STIRAP in which molecules are brought to the ground rovibrational state through a series of intermediate states in one run, which allows to minimize collisional losses in intermediate states. In Section III we discuss direct STIRAP conversion of ultracold atoms from a scattering continuum into deeply bound molecules in the presence of a Feshbach resonance. Direct conversion without first forming Feshbach molecules allows to reduce collisional losses during formation of molecules.

2. Theory of multistate chainwise adiabatic passage in the presence of decay

In this section, we present a multistate chainwise STIRAP technique allowing an efficient transfer of a molecule from a high-lying state to the ground vibrational state which minimizes the population loss due to inelastic collisions during the transfer process (30).

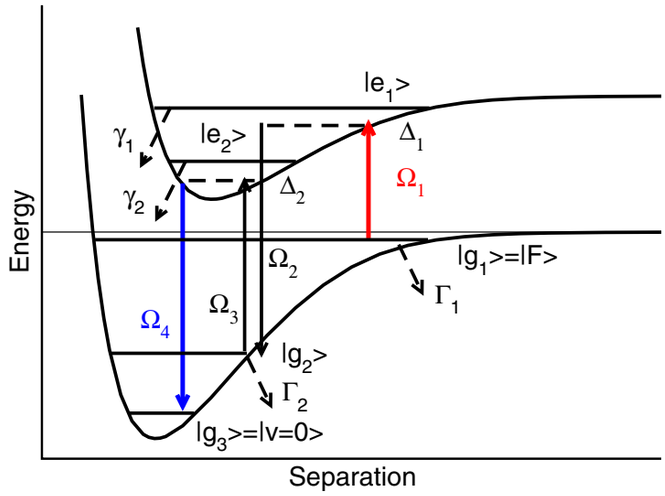

Fig. 1. Schematic showing the multistate chainwise STIRAP transfer of population from the Feshbach $|g_1\rangle$ to the ground $|g_3\rangle$ vibrational state.

We analyze a simple five-level model molecular system with states chainwise coupled by optical fields as illustrated in Fig. 1. The states $|g_1\rangle$, $|g_2\rangle$ and $|g_3\rangle$ are vibrational levels of a ground electronic molecular state, while $|e_1\rangle$ and $|e_2\rangle$ are vibrational states of an excited electronic molecular state. Molecules are formed in a high energy state $|g_1\rangle$, which in the following we assume to be a molecular Feshbach state. The state $|g_3\rangle$ is the deepest bound vibrational state $v = 0$, and $|g_2\rangle$ is an intermediate vibrational state. The goal is to efficiently transfer the population from the state $|g_1\rangle$ to state $|g_3\rangle$. At least two vibrational levels $|e_1\rangle$ and $|e_2\rangle$ in an excited electronic state are required, one which has a good Franck-Condon overlap with $|g_3\rangle$, and the other having a good overlap with the initial Feshbach molecular state $|g_1\rangle$. In the states $|e_1\rangle$ and $|e_2\rangle$, molecules decay due to spontaneous emission and collisions, and in the states $|g_1\rangle$ (for bosonic molecules) and $|g_2\rangle$ they experience fast inelastic collisions with background atoms leading to loss of molecules from a trap. It means that populating the states $|e_1\rangle$, $|e_2\rangle$ and $|g_2\rangle$ has to be avoided when a background atomic gas is present, or the transfer process has to be faster than the collisional relaxation time.
First, we analyze the system neglecting all decays. The wave function of the system is $|\Psi\rangle = \sum_i C_i \exp(-i\phi_i(t))\,|i\rangle$, where $i = g_1, e_1, g_2, e_2, g_3$; $\phi_{g_1} = 0$, $\phi_{e_1} = \nu_1 t$, $\phi_{g_2} = (\nu_2 - \nu_1)t$, $\phi_{e_2} = (\nu_3 + \nu_2 - \nu_1)t$, $\phi_{g_3} = (\nu_4 - \nu_3 + \nu_2 - \nu_1)t$; ν_i is the frequency of the ith optical field. The evolution is then governed by the Schrödinger equation

$$i\hbar \frac{\partial |\Psi\rangle}{\partial t} = H(t)\,|\Psi\rangle\,. \tag{1}$$

The time-dependent Hamiltonian of the system in the rotating wave approximation is given by

$$H(t) = \begin{pmatrix} 0 & -\Omega_4(t) & 0 & 0 & 0 \\ -\Omega_4(t) & \Delta_2 & -\Omega_3(t) & 0 & 0 \\ 0 & -\Omega_3(t) & 0 & -\Omega_2(t) & 0 \\ 0 & 0 & -\Omega_2(t) & \Delta_1 & -\Omega_1(t) \\ 0 & 0 & 0 & -\Omega_1(t) & 0 \end{pmatrix}, \tag{2}$$

where $\Omega_1(t) = \mu_1\mathcal{E}_1(t)/2\hbar$, $\Omega_2(t) = \mu_2\mathcal{E}_2(t)/2\hbar$, $\Omega_3(t) = \mu_3\mathcal{E}_3(t)/2\hbar$ and $\Omega_4(t) = \mu_4\mathcal{E}_4(t)/2\hbar$ are the Rabi frequencies of optical fields; $\mathcal{E}_i$ is the amplitude of ith optical field, μ_i is the dipole matrix element along the respective transition, $\Delta_1 = \omega_1 - \nu_1$ and $\Delta_2 = \omega_4 - \nu_4$ are one-photon detunings of the fields, and the ω_i are the molecular frequencies along transition i.

We assumed in Eq. (2) that pairs of fields coupling two neighboring ground state vibrational levels are in a two-photon (Raman) resonance; in this case, the system has a dark state, given by the expression

$$\left|\Phi^0\right\rangle = \frac{\Omega_2\Omega_4\left|g_1\right\rangle - \Omega_4\Omega_1\left|g_2\right\rangle + \Omega_1\Omega_3\left|g_3\right\rangle}{\sqrt{\Omega_4^2\Omega_1^2 + \Omega_1^2\Omega_3^2 + \Omega_2^2\Omega_4^2}}. \tag{3}$$

In c-STIRAP (as in classical STIRAP) the optical fields are applied in a counterintuitive way, *i.e.* at $t = -\infty$ only a combination of the Ω_4, Ω_3, Ω_2 fields, and at $t = +\infty$ only of Ω_3, Ω_2 and Ω_1 is present. As a result the dark state is initially associated with the $|g_1\rangle$ and finally with the $|g_3\rangle$ states. Adiabatically changing the Rabi frequencies of the optical fields so that the system stays in the dark state during its evolution, one can transfer the system from the initial high-lying $|g_1\rangle$ to the ground vibrational $|g_3\rangle$ state with unit efficiency, defined as the population of the $|g_3\rangle$ state at $t = +\infty$. The dark state does not have contributions from the $|e_1\rangle$ and $|e_2\rangle$ excited states, which means that they are not populated during the transfer process. As a result, the decay from these states does not affect the transfer efficiency. Decay from the $|g_1\rangle$, $|g_2\rangle$, $|g_3\rangle$ states will, however, degrade the coherent superposition (3) and result in population loss from the dark state and reduction of the transfer efficiency. In the next two subsections we consider two c-STIRAP schemes which can be used for efficient population transfer to the ground vibrational state with minimal population loss due to intermediate states decay.

2.1 c-STIRAP with two pulses

Two regimes can provide efficient population transfer to the ground state using multiple intermediate states. In the first one, called c-STIRAP, as also proposed in (31), the Stokes pulses Ω_2 and Ω_4 are applied simultaneously followed with a delay by pump pulses Ω_1 and Ω_3, applied at the same time as well. It means that, ideally, only two pulses can be used so that $\Omega_2(t) = \Omega_4(t) = \Omega_s(t)$ are Stokes pulses and $\Omega_1(t) = \Omega_3(t) = \Omega_p(t)$ are pump pulses. To simplify the analysis, we set the one-photon detunings to zero $\Delta_1 = \Delta_2 = 0$, and define an effective Rabi frequency $\Omega(t) = \sqrt{\Omega_p(t)^2 + \Omega_s(t)^2}$ and a rotation angle $\theta(t)$ by $\tan\theta = \Omega_p/\Omega_s$. In this case the Hamiltonian (2) has a zero eigenvalue describing the dark state (3). Four other eigenvalues correspond to bright states and are given in Appendix A along with a rotation matrix W converting adiabatic eigenstates into the bare ones. To study the effect of the decay from the intermediate state $|g_2\rangle$ and the initial state $|g_1\rangle$ on the dark state evolution, we turn to a density matrix description (32). The density matrix equation taking into account decay in the bare state basis is

$$i\hbar\frac{d\rho}{dt} = [H,\rho] - \mathcal{L}\rho, \tag{4}$$

where the Liouville operator $\mathcal{L}$ consists of the usual decays (see exact form in the Appendix A), where only population decays ($\propto T_1^{-1}$) into other vibrational states or the continuum are considered. Initially, all population is assumed to be in state $|g_1\rangle$.

It is convenient to use the adiabatic basis states to study the effect of decay. In the adiabatic basis the density matrix equation (4) transforms into

$$i\hbar\frac{d\rho^a}{dt} = [H^a, \rho^a] - i\hbar\left[W^T\dot{W}, \rho^a\right] - \mathcal{L}^a\rho^a \tag{5}$$

where the density matrix and the Liouville operator in this basis are given by $\rho^a = W^T\rho W$ and $\mathcal{L}^a\rho^a = W^T\mathcal{L}\rho W$, and the Hamiltonian H^a is diagonal; W is the rotation matrix, given by (A1) in the Appendix A. Initial conditions for Eq. (5) read as $\rho^a_{00} = 1$, $\rho^a_{nm} = 0$ for $n, m \neq 0$, where ρ^a_{00} denotes the dark state population. The second term on the right hand side of Eq. (5) is responsible for non-adiabatic couplings. This term results in excitation of nondiagonal density matrix elements due to coupling with the dark state. Since the nondiagonal elements ρ^a_{0i}, $i = 0, ..4$, are excited first, the second term in the r.h.s. of Eq. (5), which is $\propto \dot{\theta}\rho^a_{00}$, has to be much smaller than the first term $\sim |\varepsilon_0 - \varepsilon_i|\rho^a_{0i}$ to keep these non-diagonal elements negligible. Thus, in order to maintain adiabaticity for the system to stay in the dark state during the transfer process, we must have

$$\dot{\theta} \ll |\varepsilon_0 - \varepsilon_{1,2}|\,,\ |\varepsilon_0 - \varepsilon_{3,4}|\,. \tag{6}$$

This gives a standard STIRAP adiabaticity requirement $\Omega T_{\rm tr} \gg 1$, where $T_{\rm tr}$ is the c-STIRAP transfer time.
From Eq. (5), the density matrix equation for the dark state population in terms of density matrix elements in the bare state basis can be written as

$$\begin{aligned}\dot{\rho}^a_{00}/\xi = &-\Gamma_1\cos^4\theta\rho_{g_1g_1} - \Gamma_2\sin^2\theta\cos^2\theta\rho_{g_2g_2} + \\ &+\frac{1}{2}\Big((\Gamma_2+\Gamma_1)\sin\theta\cos^3\theta\rho_{g_1g_2} + \Gamma_2\cos\theta\sin^3\theta\rho_{g_2g_3} - \Gamma_1\sin^2\theta\cos^2\theta\rho_{g_1g_3} + c.c.\Big)\end{aligned} \tag{7}$$

with $\xi = (1 - \frac{1}{4}\sin^2 2\theta)^{-1}$. Provided that the transfer is adiabatic, so that the system stays in the dark state during the evolution: $\rho^a_{00} \approx 1$, the density matrix elements in the bare state basis appearing in (7) are expressed via the dark state population in the following way:

$$\begin{aligned}\rho_{g_1g_1} &\approx \rho^a_{00}\,\xi\,\cos^4\theta,\\ \rho_{g_2g_2} &\approx \rho^a_{00}\,\xi\,\sin^2\theta\cos^2\theta,\\ \mathrm{Re}\left(\rho_{g_1g_2}\right) = \mathrm{Re}\left(\rho_{g_2g_1}\right) &\approx -\rho^a_{00}\,\xi\,\sin\theta\cos^3\theta,\\ \mathrm{Re}\left(\rho_{g_2g_3}\right) = \mathrm{Re}\left(\rho_{g_3g_2}\right) &\approx -\rho^a_{00}\,\xi\,\cos\theta\sin^3\theta,\\ \mathrm{Re}\left(\rho_{g_1g_3}\right) = \mathrm{Re}\left(\rho_{g_3g_1}\right) &\approx \rho^a_{00}\,\xi\,\sin^2\theta\cos^2\theta.\end{aligned}$$

Inserting these back into Eq. (7), one obtains the equation describing the dark state population decay

$$\dot{\rho}^a_{00} \approx -\left(\Gamma_1\cos^4\theta + \Gamma_2\sin^2\theta\cos^2\theta\right)\xi\rho^a_{00}. \tag{8}$$

As expected, the dark state is not affected by the decay from the excited states $|e_{1,2}\rangle$, but only by the decay from the states $|g_{1,2}\rangle$, which destroys the coherent superposition the dark state is based on.
Taking Gaussian laser pulses with the pump and Stokes pulse Rabi frequencies $\Omega_p = \Omega_0 \exp\left(-(t-\tau/2)/T^2\right)$ and $\Omega_S = \Omega_0 \exp\left(-(t+\tau/2)/T^2\right)$ with $\tan\theta = \exp\left(2t\tau/T^2\right)$, one can see that at the moment $t = 0$ of maximal interaction the rotation angle is $\theta = \pi/4$. The density matrix equation (8) then takes a form

$$\dot{\rho}^a_{00} = -\rho^a_{00}(\Gamma_1 + \Gamma_2)/3. \tag{9}$$

Equation (9) shows that in this regime the decay of both the initial and intermediate vibrational states is not suppressed, *i.e.* directly influences the dark state evolution. This scheme therefore can be applied only if $\Gamma_{1,2} T_{\rm tr} \ll 1$. It implies that c-STIRAP pulses have to be shorter than the collisional relaxation time. This requirement combined with the adiabaticity condition might result in large Rabi frequencies needed for high transfer effciency. However, as will be shown in the next section, using reasonable values of Rabi frequencies (~ 10 MHz) and pulse durations, rather high transfer efficiencies of the order of 90% and 85% for fermionic and bosonic alkali dimers, respectively, can be realized in this scheme in the presence of collisions. High transfer efficiency with weaker and longer pulses is possible in this scheme if the remaining atoms are removed after the molecules are formed. It can be done by applying a "blast" laser pulse resonant with an atomic, but not a molecular electronic transition. In this case $\Gamma_{1,2}$ are determined by vibrationally inelastic molecule-molecule collisions, which result in slower decay compared to atom-molecule collisions due to a typically smaller density of molecules. Although, it is worth noting that in this case a collision results in two molecules lost from a trap. Another situation when this regime gives high transfer efficiency using weaker pulses can be used is when molecules are formed in an optical lattice with initially two atoms per site. In this case $\Gamma_{1,2}$ will be determined by off-resonant Raman scattering of lattice and STIRAP laser fields (25), which can be sufficiently suppressed.

2.2 Chainwise "straddling" STIRAP

As we discussed in the previous subsection, if the remaining atoms are not removed from the trap, the molecules in the $|g_{1,2}\rangle$ states are subject to vibrationally inelastic atom-molecule collisions. To maximaize the number of molecules transferred to the ground $|g_3\rangle$ state the population of the decaying intermediate state $|g_2\rangle$ has to be minimized. This can be achieved using an extension of the STIRAP technique to multiple chainwise-coupled states, called a "straddling" STIRAP (33). Namely, if Ω_2, $\Omega_3 \gg \Omega_1$, Ω_4 and Ω_2, Ω_3 temporally overlap both the Ω_1 and Ω_4 pulses, populations in all intermediate states are minimized. To simplify the analysis, we assume $\Omega_2 = \Omega_3 = \Omega_0$; Ω_0 is independent of time (in practice the corresponding pulses just have to be much longer than $\Omega_1(t)$, $\Omega_4(t)$ and overlap both of them), and $\Omega_0 \gg |\Omega_1|, |\Omega_4|$. As in the previous subsection, we set one-photon detunings to zero $\Delta_1 = \Delta_2 = 0$, and define the effective Rabi frequency $\Omega(t) = \sqrt{\Omega_1(t)^2 + \Omega_4(t)^2}$ and a rotation angle by $\tan\theta(t) = \Omega_1(t)/\Omega_4(t)$. The eigenvalues of the system (2) are $\varepsilon_0 = 0$, corresponding to the dark state, and $\varepsilon_{1,2} = \pm\Omega/\sqrt{2}$, and $\varepsilon_{3,4} = \pm\sqrt{2}\Omega_0$ to bright states. Adiabatic eigenstates $|\Phi\rangle = \{|\Phi^n\rangle\}$, $n = 0, ...4$ and the bare states $|\Psi\rangle = \left\{\left|\Psi^l\right\rangle\right\}$, $l = g_1, e_1, g_2, e_2, g_3$ are transformed via a rotation matrix (A2), given in the Appendix A.

The adiabaticity condition (6) in this case becomes $\dot{\theta} \ll \Omega,\ \Omega_0$. If the condition $\dot{\theta} \ll \Omega$ is satisfied, the dark state will not couple to the $\left|\Phi^{1,2}\right\rangle$ states. Coupling to the $\left|\Phi^{3,4}\right\rangle$ states will be suppressed even more strongly, since $\Omega \ll \Omega_0$.
The density matrix equation for the dark state population in terms of density matrix elements in the bare state basis in this case is given by

$$\begin{aligned}\dot{\rho}^a_{00} &= \Gamma_1 \cos^2\theta \rho_{g_1g_1} - \Gamma_2 \left(\frac{\Omega \sin 2\theta}{2\Omega_0}\right)^2 \rho_{g_2g_2} + \\ &+ \left(\Gamma_2 \frac{\Omega}{4\Omega_0} \sin 2\theta \sin\theta \rho_{g_2g_3} + \frac{\Gamma_1}{2} \sin\theta \cos\theta \rho_{g_1g_3} + \right. \\ &\left. + (\Gamma_1 + \Gamma_2) \frac{\Omega}{2\Omega_0} \sin 2\theta \cos\theta \rho_{g_1g_2} + c.c.\right) . \end{aligned} \tag{10}$$

For adiabatic evolution $\rho^a_{00} \approx 1$, and the density matrix elements in the bare state basis are expressed via the dark state population as:

$$\rho_{g_2g_2} \approx \sin^2 2\theta \frac{\Omega^2}{4\Omega_0^2} \rho^a_{00},$$

$$\mathrm{Re}\left(\rho_{g_1g_2}\right) = \mathrm{Re}\left(\rho_{g_2g_1}\right) \approx -\frac{\Omega}{2\Omega_0} \sin 2\theta \cos\theta \rho^a_{00},$$

$$\mathrm{Re}\left(\rho_{g_2g_3}\right) = \mathrm{Re}\left(\rho_{g_3g_1}\right) \approx -\frac{\Omega}{2\Omega_0} \sin 2\theta \sin\theta \rho^a_{00},$$

$$\mathrm{Re}\left(\rho_{g_1g_3}\right) = \mathrm{Re}\left(\rho_{g_3g_1}\right) \approx \sin 2\theta \rho^a_{00}/2.$$

The decay of the dark state due to the population loss from the $|g_1\rangle$ and $|g_2\rangle$ states is then described by the equation (keeping only terms up to the Ω^2/Ω_0^2 order)

$$\dot{\rho}^a_{00} \approx -\left((\Gamma_2 + \Gamma_1 \cos^2\theta)\left(\frac{\Omega}{2\Omega_0} \sin 2\theta\right)^2 + \Gamma_1 \cos^2\theta\right) \rho^a_{00} . \tag{11}$$

Equation (11) shows that intermediate state decay can be neglected during the transfer time T_{tr} if $(\Gamma_1 + \Gamma_2) T_{\mathrm{tr}} \left(\sin 2\theta \Omega/2\Omega_0\right)^2 \ll 1$. From this expression one can see that the intermediate state decay rate is reduced by a factor $(\Omega/\Omega_0)^2 \ll 1$ in this regime. It also follows from Eq. (11) that decay from the initial state $|g_1\rangle$ is not suppressed, so that the transfer process has to be faster than this decay.
Both schemes can be readily extended to a general N-state chainwise-linked system with odd number of states having $(N+1)/2$ ground and $(N-1)/2$ excited levels (33; 34). In the two-pulse STIRAP scheme, considered in the previous subsection, all Stokes pulses are applied simultaneously followed with a delay by pump pulses applied at the same time as well. In the second regime counterintuitively ordered pump and Stokes pulses drive the first and the last transitions in the chain, while intermediate states are coupled by strong CW (or pulsed with durations longer than that of the pump and Stokes pulses) fields. In the

second regime analyzed in this subsection the population of all intermediate states is strongly suppressed, and the transfer efficiency close to unity can be realized.
The major prerequisite for high transfer efficiency in STIRAP is the two-photon resonance between fields coupling vibrational levels in the ground electronic state via Raman transitions. It requires all fields to be phase coherent. In a general case the frequency difference between any fields in the chain can be in the THz range. To maintain phase coherence at these large frequency differences the fields can then be phase locked to an optical frequency comb (35).

2.3 Collisional relaxation rates for fermionic and bosonic alkali dimers

Magneto- and photo-association techniques produce molecules mostly from ultracold Bose, two-spin component Fermi and mixture alkali metal atomic gases. Weakly bound Feshbach molecules rapidly decay due to vibrationally inelastic atom-molecule collisions, which were found to be the major molecule lifetime limiting factor in atomic traps. Depending on the quantum statistics due to the nuclear spin of the constituent atoms, the alkali dimers show different behavior with respect to inelastic atom-molecule and molecule-molecule collisions. Fermionic alkali dimers in the Feshbach state are very stable with respect to collisions. They are particularly stable close to the resonance, where the scattering length is large. The stability of the fermionic molecules has been explained based on the Pauli exclusion principle combined with significantly different length scales associated with the initial and final vibrational states (36). Lifetimes of the Feshbach molecular states of the order of 1 s have been observed experimentally for $^6Li_2$ fermionic molecules (37; 38), giving $\Gamma_1 \sim 1\ s^{-1}$, and of the order of 100 ms for $^{40}K_2$ molecules (39), giving $\Gamma_1 \sim 10\ s^{-1}$. More deeply bound Feshbach molecules have larger decay rates, with the corresponding collision coefficient $k_{inel} \sim 10^{-11}\ cm^3s^{-1}$. With typical densities of atoms in traps $n_{at} \sim 10^{11} - 10^{14}\ cm^{-3}$, it gives $\Gamma_1 = k_{inel} n_{at} \sim (1 - 10^3)\ s^{-1}$ for these molecules. To calculate the intermediate state decay rate Γ_2 we use results of a theoretical analysis of collisional stability of low-lying vibrational states of fermionic and bosonic Li_2 molecules (40). In low vibrational states, as was shown, fermionic molecules experience fast vibrational quenching due to collisions with surrounding atoms, leading to loss of both molecules and atoms from a trap. The inelastic atom-molecule collision coefficient for fermionic molecules in these low vibrational states is of the order of $k_{inel} \sim 3 \cdot 10^{-10}\ cm^3s^{-1}$ (calculated in Ref.(40) for fermionic $^6Li_2$ in $v = 1$). The vibrational relaxation rate Γ_2 can then be estimated using $n_{at} \sim 10^{11} - 10^{14}\ cm^{-3}$, giving $\Gamma_2 = k_{inel} n_{at} \sim 3 \cdot (10^1 - 10^4)\ s^{-1}$.
In contrast to fermionic alkali dimers, bosonic dimers experience fast vibrational quenching due to inelastic atom-molecule collisions, even in their Feshbach state. As was observed experimentally for ^{23}Na (41) and ^{133}Cs (42), the inelastic collision coefficient for bosonic molecules due to atom-molecule collisions is of the order of $k_{inel} \sim 5 \cdot 10^{-11}\ cm^3s^{-1}$ for the Feshbach state. An inelastic atom-molecule collision coefficient $k_{inel} \sim 10^{-10}\ cm^3s^{-1}$ and an elastic collision coefficient of the same order have been theoretically predicted for $^{87}Rb_2$ molecules for magetic fields below the Feshbach 1007.4 G resonance (43). Fast vibrationally inelastic atom-molecule collisions thus limit the lifetime of the molecules in the trap to 100 μs - 1 ms. They also limit the atom-to-molecule conversion efficiency during the magnetic field ramp across the resonance. The lifetime of the bosonic molecules in the trap can be significantly extended if at the end of the magnetic field ramp a "blast" laser pulse is applied, selectively removing atoms from the trap (41). In this case, the main loss mechanism is vibrationally inelastic molecule-molecule collisions. The corresponding collision coefficient

Two-pulse c-STIRAP		"Straddling" STIRAP	
$1 \ll$	$\Omega T_{\rm tr}$	$1 \ll$	$\Omega T_{\rm tr} \ll \frac{\Omega_0^2}{\Omega\Gamma_2}$
$\Omega \sim$	$E_{\rm Fesh}$	$\Omega \sim$	$E_{\rm Fesh}$
$1 \gg$	$\Gamma_{1,2} T_{\rm tr}$	$1 \gg$	$\Gamma_1 T_{\rm tr}$

Table 1

in the Feshbach state was measured for a bosonic $^{23}Na_2$ molecule as $k_{\rm inel} \sim 5.1 \cdot 10^{-11}$ cm^{3}s^{-1} (41). In this experiment, the initial atomic density and the atom-to-molecule conversion efficiency were $n_{\rm at} \sim 1.7 \cdot 10^{14}$ cm^{-3} and 4%, respectively, giving the molecular density of $n_{\rm mol} \sim 6 \cdot 10^{12}$ cm^{-3} and therefore the decay rate $\Gamma_1 = k_{\rm inel} n_{\rm mol} \sim 300$ s^{-1}. The vibrational relaxation rate Γ_2 of intermediate vibrational states for bosonic molecules can be estimated from the inelastic atom-molecule collision coefficient in low vibrational states $k_{\rm inel} \sim 6 \cdot 10^{-10}$ cm^{3}s^{-1} (calculated in Ref.(40) for bosonic ^{7}Li in $v = 1$). For a typical density of atoms in a trap, $n_{\rm at} \sim 10^{11} - 10^{14}$ cm^{-3} and the resulting relaxation rate is $\Gamma_2 \sim 6 \cdot (10^1 - 10^4)$ s^{-1}.
The heteronuclear molecules are formed from a mixture of Bose and Fermi atomic gases, and their collisional properties are expected to differ from pure fermionic and bosonic molecules discussed above. Stability of the KRb molecules with respect to collisions with initial fermionic and bosonic atoms has been recently studied in (44). Vibrationally inelastic relaxation was found to be dominated by atom-molecule collisions, and the corresponding collision coefficients to strongly depend on the quantum statistics of the atoms. Close to the heteronuclear Feshbach resonance the collision coefficient for collisions with indistinguishable fermions (^{40}K in the same hyperfine state) was found to be $k_{\rm inel} < 10^{-11}$ cm^{3}s^{-1}; for collisions with indistinguishable bosons (^{87}Rb in the same hyperfine state) $k_{\rm inel} \sim (2-3) \cdot 10^{-10}$ cm^{3}s^{-1} close to the resonance. Finally, for collisions with distinduishable atoms (^{40}K in a different hyperfine state) the collision coeffcient $k_{inel} \sim (3-5) \cdot 10^{-11}$ cm^{3}s^{-1} was measured. These results are therefore consistent with coefficients of vibrationally inelastic collisions with pure fermionic and bosonic atoms, considered in previous paragraphs.
Let us now estimate the parameters of the optical pulses providing maximal transfer efficiency. As follows from Eqs. (3) and Eq. (11), in both STIRAP schemes the decay of the Feshbach state strongly affects the transfer efficiency, and the condition $\Gamma_1 T_{\rm tr} \ll 1$ has to be satisfied to minimize molecular loss. At the same time the adiabaticity condition requires $\Omega T_{\rm tr} \gg 1$. Weakly bound Feshbach states are very close to a dissociation threshold, a typical binding energy $E_{\rm Fesh}$ being tens kHz -tens MHz (~ 1 μK - 1 mK). At these small binding energies the first pulse in the chain (Ω_p or Ω_1 in the two STIRAP schemes), coupling the Feshbach state $|g_1\rangle$ to the first excited state $|e_1\rangle$ can lead to back-action, *i.e.* back transfer of the molecule to the scattering contunuum, thus molecular dissociation, via a stimulated Raman process. This effect is minimized if the binding energy of a molecule $E_{\rm Fesh}$ is much larger than the effective Rabi frequency corresponding to the coupling between the $|e_1\rangle$ state and the scattering continuum. Typically, the dipole moment of the bound-bound transition greatly exceeds the dipole moment of the bound-continuum transition. Therefore, the Rabi frequency of the $\mathcal{E}_1$ field between the bound-bound transition $|g\rangle_1 - |e\rangle_1$ will be much larger than the effective Rabi frequency for the same field corresponding to coupling between the $|e_1\rangle$ and the scattering continuum. It means that choosing $\Omega \sim E_{\rm Fesh}$ one can make the back transfer process negligible. Finally, we have the following requirements for the Rabi frequencies and durations of the STIRAP pulses (amplitudes and durations are assumed the same for the Stokes and the pump pulse to maximize the transfer efficiency).

The set of requirements in the table 1 allows one to obtain a general range of Rabi frequencies and pulse durations, providing optimal population transfer. Since the goal is the production of dense molecular gases with a large number of molecules, we consider a high initial atomic density $n_{\rm at} \sim 10^{14}$ cm^{-3} in a trap in our estimates. For bosonic molecules the inelastic atom-molecule collision coefficient differs at resonance and for deeper bound Feshbach molecules by about a factor of two, giving $\Gamma_1 \sim 5 \cdot 10^3 - 10^4$ s^{-1} at this density. One can see that the c-STIRAP transfer time has be $T_{\rm tr} \ll 10^{-4}$ s. Adiabaticity typically requires $\Omega T_{\rm tr} \sim 10^2$, giving a lower limit on the Rabi frequencies of the c-STIRAP pulses $\Omega \gg 10^6$ s^{-1}. As our analysis shows transfer efficiencies $> 90\%$ can be achieved with pulse durations of several μs and Rabi frequencies of $5 - 10$ MHz. It means that to minimize dissociation of molecules due to the back transfer deeper bound Feshbach molecules with $E_{\rm Fesh} > 1$ MHz are prefered. For deeper bound fermionic molecules the decay rate $\Gamma_1 \sim 10^3$ s^{-1} at this high atomic density, resulting in the same pulse durations and Rabi frequencies, maximizing the transfer efficiency, as for bosonic molecules. At resonance, fermionic molecules have significantly smaller decay rates $\Gamma_1 \sim 1 - 10$ s^{-1}. In this case high transfer efficiencies $> 90\%$ can be realized with longer and weaker pulses of hundred μs duration and Rabi frequencies ~ 1 MHz.

Next we illustrate the technique with numerical simulations of a transfer process based on the system (4) for model seven-state bosonic and fermionic molecular systems. A seven-state system shown in Fig. 2a is easier to realize experimentally, *i.e.* to find transitions with good Franck-Condon factors, than the five-level scheme, analyzed in the previous subsection. For example, a seven-state chainwise path from the Feshbach to the ground vibrational state was found in $^{87}Rb_2$. The Feshbach state is experimentally formed after a magnetic field crosses the Feshbach resonance at 1007.4 G. Far from the resonance at 973 G the Feshbach state binding energy is 24 MHz (25). In the first step it can be coupled to an electronically excited pure long range molecular state $\left|0_g^-, v, J=0\right\rangle$, located close to the $5S_{1/2} + 5P_{3/2}$ dissociation asymptote (45). For example, $v = 31$ vibrational level can be chosen located 6.87 cm^{-1} (≈ 206 GHz) below the asymptote. The corresponding Rabi frequency scales with the field intensity as $\Omega_1 = 2\pi \times 2.9\sqrt{I(W/cm^2)}$ s^{-1}, giving the transition dipole moment $\mu_1 \sim 0.3$ D. The second transition of the STIRAP scheme in (25) was to the second-to-last bound vibrational state, located 637 MHz below the ground electronic state dissociation asymptote. The corresponding Rabi frequency scales as $\Omega_2 = 2\pi \times 6\sqrt{I(W/cm^2)}$ s^{-1}, giving the transition dipole moment $\mu_2 \sim 0.6$ D. The authors mention that the Franck-Condon factors from the excited $\left|0_g^-, v=31, J=0\right\rangle$ state to the ground state vibrational levels down to the $X\ ^1\Sigma_g^+(v = 116)$ are similar to the second-to-last vibrational state. This includes the $X\ ^1\Sigma_g^+(v = 119)$ from where the ground vibrational state can be reached in five steps (29):

$$
\begin{aligned}
X\ ^1\Sigma_g^+(v=119, J=0) &\rightarrow A^1\Sigma_u^+(v'=185, J=1),\\
A\ ^1\Sigma_u^+(v'=185, J=1) &\rightarrow X^1\Sigma_g^+(v=52, J=0),\\
X\ ^1\Sigma_g^+(v=52, J=0) &\rightarrow A^1\Sigma_u^+(v'=24, J=1),\\
A\ ^1\Sigma_u^+(v'=24, J=1) &\rightarrow X^1\Sigma_u^+(v=0, J=0).
\end{aligned}
$$

The results of the numerical solution of the density matrix equation (4) for a fermionic molecular system are given in Fig. 2. The left column presents the maximal transfer efficiency

case for the the two-pulse c-STIRAP scheme, and the right column for the "straddling" STIRAP scheme. In the two-pulse c-STIRAP scheme, the states $|g_1\rangle - |e_1\rangle$; $|g_2\rangle - |e_2\rangle$; $|g_3\rangle - |e_3\rangle$ are coupled by the pump field $\Omega_p = \Omega_p^{\max}(1 + \tanh(t - \tau/2)/T)/2$, while the states $|e_1\rangle - |g_2\rangle$; $|e_2\rangle - |g_3\rangle$; $|e_3\rangle - |g_4\rangle$ are coupled by the Stokes field $\Omega_S = \Omega_S^{\max}(1 - \tanh(t + \tau/2)/T)/2$. In the "straddling" STIRAP scheme the states $|e_1\rangle - |g_2\rangle$; $|g_2\rangle - |e_2\rangle$, $|e_2\rangle - |g_3\rangle$; and $|g_3\rangle - |e_3\rangle$ are coupled by CW laser fields with a Rabi frequency Ω_0, the first transition $|g_1\rangle - |e_1\rangle$ and the last transition $|e_3\rangle - |g_4\rangle$ in the chain are coupled by the fields $\Omega_1 = \Omega_1^{\max}(1 + \tanh(t - \tau/2)/T)/2$ and $\Omega_4 = \Omega_4^{\max}(1 - \tanh(t + \tau/2)/T)/2$, respectively. The transfer efficiency does not strongly depend on the form of optical pulses in this case, the same transfer efficiency was obtained using Gaussian pulses. In the numerical analysis a deeper bound Feshbach state with $E_{\text{Fesh}} \sim$ tens MHz was assumed, which was the case in the $^{87}Rb_2$ STIRAP experiment (25). The Rabi frequencies of STIRAP fields were chosen to satisfy the second condition of the 1, and the pulse duration T and delay τ were varied to find the maximal transfer efficiency. To estimate the decay rate of intermediate vibrational states, the atomic density $n_{\text{at}} \sim 10^{14}$ cm^{-3} was used along with the inelastic collision coefficient $k_{\text{inel}} \sim 3 \cdot 10^{-10}$ cm^{3}s^{-1}, giving $\Gamma_{2,3} = 3 \cdot 10^4$ s^{-1}. Lifetimes of vibrational states of an excited electronic state of the order of 30 ns ($\gamma_{1,2,3} = 3 \cdot 10^7$ s^{-1}) were also assumed.

The numerical analysis demonstrates that $>$ 90% of population in the case of two-pulse c-STIRAP (see Fig. 2d) and $>$ 96% in the case of "straddling" STIRAP (see Fig. 2e) can be transfered from the Feshbach to the ground vibrational state for the chosen Rabi frequencies using the two-pulse and "straddling" STIRAP schemes, respectively, even in the presence of fast collisional decay of the Feshbach state. This transfer efficiency is realized using STIRAP pulses much shorter than the Feshbach state lifetime. Thus the influence of the decay of this state is significantly reduced.

Results of a similar analysis for a model seven-level bosonic molecular system are shown in Fig. 3. Transfer efficiency of the order of 85% and 92% can be realized with the two-pulse and "straddling" STIRAP schemes, respectively. In this case the form of the STIRAP pulses plays an important role due to the fast decay of the Feshbach state. Using Gaussian pulses instead of tanh pulses results in significantly smaller transfer efficiency since by the time the Stokes pulse arrives the Feshbach state experiences noticable decay. With tanh pulses it is, however, possible to make the delay time between the moment of molecule formation and the start of the transfer process reasonably small to minimize the Feshbach state decay.

We can now estimate intensities of CW and pulsed fields corresponding to Rabi frequencies used in our calculations. Typical dipole moments of electric dipole-allowed transitions between molecular electronic states are of the order of 1 D (Debye) and larger. Assuming that the chosen transitions have reasonably large Franck-Condon factors, we use an estimate of transition dipole moments between vibrational levels in the ground and excited electronic state $D_{v,v'} \sim 1$ D. Taking the peak Rabi frequency of the pump and Stokes fields $\Omega_{1,4}^{\max\, max} = 3 \cdot 10^7$ s^{-1}, the corresponding intensity is $I_{1,4}^{\text{peak}} = c\mathcal{E}_{1,4}^2/4\pi = c(\Omega_{1,4}^{\max}\hbar/D_{v,v'})^2/4\pi \sim 0.2$ W/cm^2; for CW fields with a Rabi frequency $\Omega_0 = 6 \cdot 10^7$ s^{-1} the corresponding intensity is $I_{2,3} \sim 0.9$ W/cm^2.

To conclude this section, we analyzed a method to coherently transfer ultracold molecules formed in high-lying vibrational states to the ground vibrational state, based on the multilevel chainwise STIRAP technique. Molecules are transfered from a high vibrational state into a ground rovibrational state $v = 0, J = 0$ using Raman transitions via several intermediate vibrational states in the ground electronic state. The former one has lower transfer efficiency

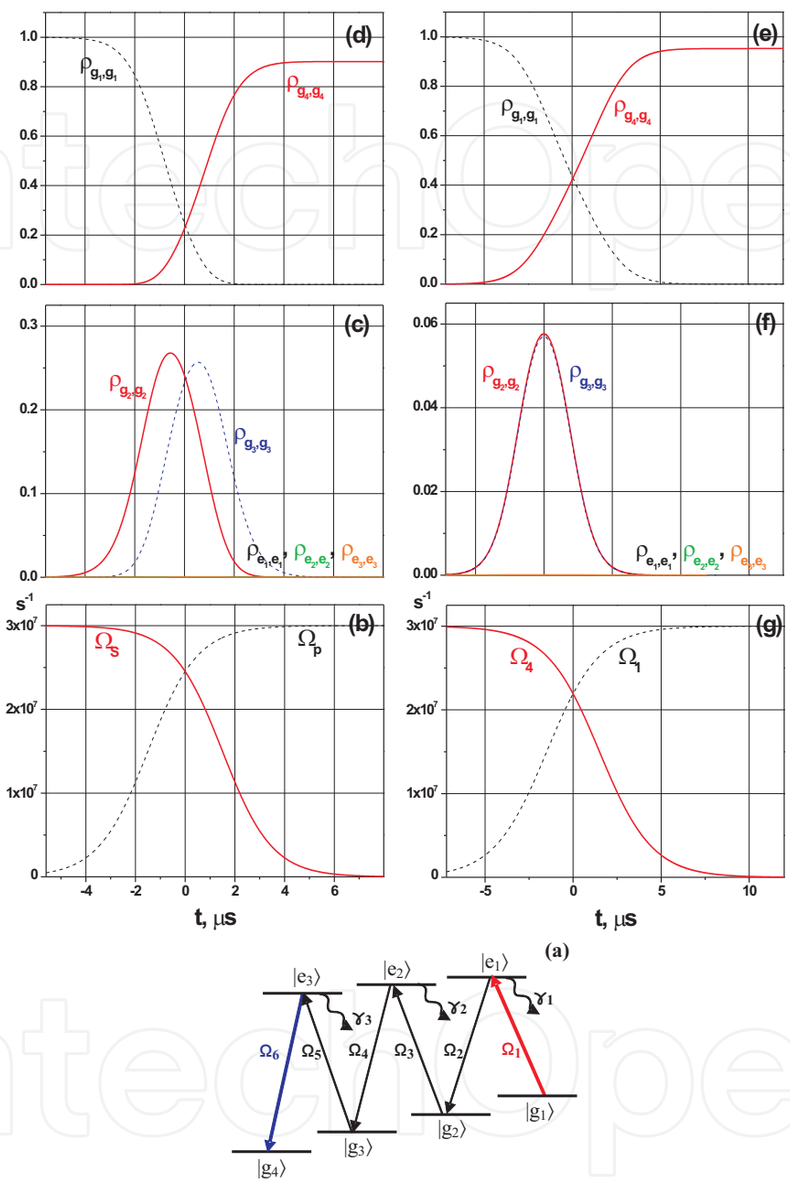

Fig. 2. Results of numerical solution of Eq. (4) for a seven-state model fermionic molecular system, shown in (a). Left colunm (figures (b),(c),(d)) and right column (figures ((e),(f),(g))) present results for a two-pulse and "straddling" STIRAP schemes, respectively. Parameters used: $\Gamma_1 = 10^3$ s^{-1}, $\Gamma_2 = \Gamma_3 = 3 \cdot 10^4$ s^{-1}, $\gamma_1 = \gamma_2 = \gamma_3 = 3 \cdot 10^7$ s^{-1}; for a two-pulse STIRAP $\Omega_p^{\max} = \Omega_S^{\max} = 3 \cdot 10^7$ s^{-1}, $T = 2$ μs, $\tau = -3$ μs; for "straddling" STIRAP $\Omega_1^{\max} = \Omega_4^{\max} = 6 \cdot 10^6$ s^{-1}, $\Omega_0 = 6 \cdot 10^7$ s^{-1}, $T = 3$ μs, $\tau = -3$ μs.

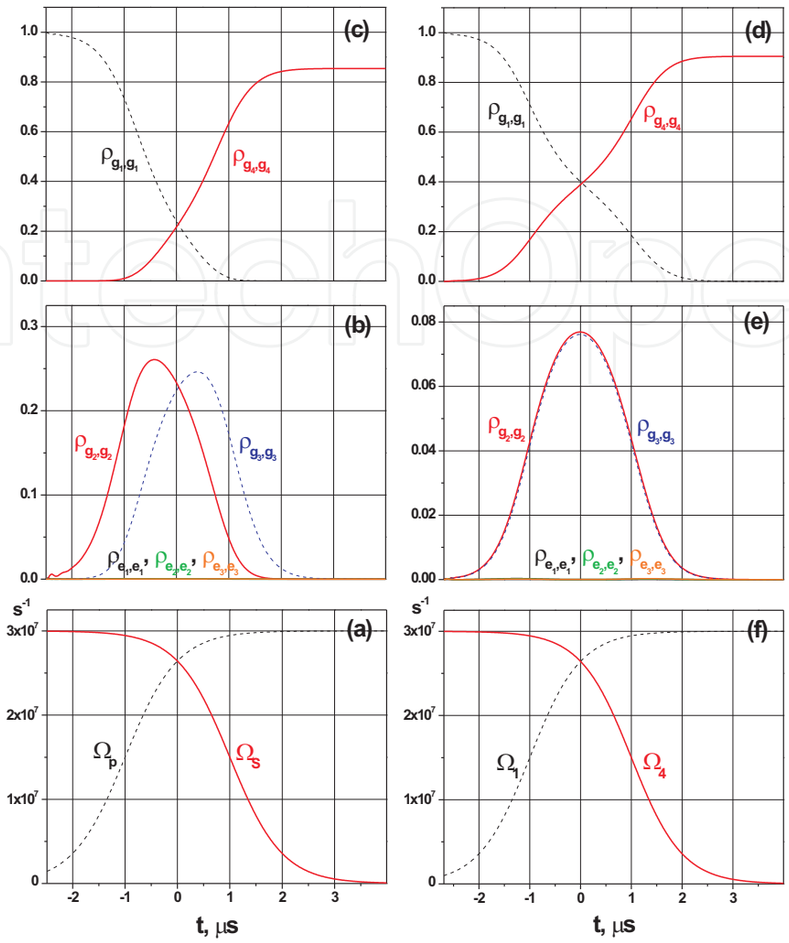

Fig. 3. Results of numerical solution of Eq. (4) for a model seven-state bosonic molecular system. Parameters used: $\Gamma_1 = 10^4$ s^{-1}, $\Gamma_2 = \Gamma_3 = 6 \cdot 10^4$ s^{-1}, $\gamma_1 = \gamma_2 = \gamma_3 = 3 \cdot 10^7$ s^{-1}; for a two-pulse STIRAP $\Omega_p^{\max} = \Omega_S^{\max} = 3 \cdot 10^7$ s^{-1}; for "straddling" STIRAP $\Omega_1^{\max} = \Omega_4^{\max} = 3 \cdot 10^7$ s^{-1}, $\Omega_0 = 6 \cdot 10^7$ s^{-1}, $T = 1$ μs, $\tau = -2$ μs for both schemes.

for both fermionic and bosonic molecules compared to the "straddling" scheme, but is experimentally simpler, since it can be realized with two pulses, while the "straddling" scheme requires at least three optical fields (two pulsed and one CW). Numerical analysis of the transfer process for a typical bosonic and fermionic molecular system in a trap with an atomic density $n_{at} \sim 10^{14}$ cm^{-3} shows that transfer efficiencies $\sim 92\%$ and $\sim 96\%$ respectively are possible even in the presence of fast collisional relaxation of the Feshbach molecular state.

Multistate chainwise STIRAP, as described in subsection 2.2, has been recently used in the Innsbruck experiment to transfer Cs_2 molecules from a Feshbach to the ground rovibrational state. The transfer efficiency of 55% has been achieved, limited by insufficient laser field intensities resulting in imperfect adiabaticity of the transfer and finite laser linewidth.

The multistate chainwise STIRAP technique allows one to use various transitions, coupled by *e.g.* rf fields and DC interactions. It can therefore be used in combination with the recently demonstrated resonant association method, where a pair of atoms is converted into

a molecule using a magnetic field modulated at a frequency close to a binding frequency of a Feshbach molecule (46). Another possibility, which we discuss in the next section, is to use the magnetic field dependent DC interchannel coupling between an entrance and a closed channel states as a first transition in the STIRAP chain (47) followed by optical transitions to the ground vibrational state. The first transition in these cases will directly couple the continuum states of colliding atoms and either a Feshbach molecular state or a bound state in the closed channel. As a result the overall atom-to-molecule conversion efficiency is expected to be higher compared to the two-step conversion sequence, when first a Feshbach molecular state is created, from where a molecule is transferred to the ground vibrational state. The chainwise STIRAP can be applied to resonant photoassociation as well, then the first transition in the STIRAP chain will couple the continuum states to a high energy vibrational state in the ground electronic state (48).

3. Efficient formation of ground state ultracold molecules via STIRAP from the continuum at a Feshbach resonance

In this section we describe photoassociative Stimulated Raman Adiabatic Passage (STIRAP) near a Feshbach resonance in a thermal atomic gas (49). We show that it is possible to use *low intensity* laser pulses to directly excite pairs of atoms in the continuum near a Feshbach resonance and to transfer nearly the entire atomic population to the lowest rovibrational level of the molecular ground state. This differs from the STIRAP techniques used in creation of ground state KRb (23) and Cs_2 (24) molecules in that the formation process starts directly from the atomic scattering continuum, avoiding formation of Feshbach molecules.

Feshbach molecules, used in the STIRAP transfer of KRb and Cs_2 to the ground rovibrational state (23; 24) are usually short-lived because of inelastic collisions with background atoms or other molecules. This is especially true for those produced from bosonic or mixed bosonic/fermionic atoms, for which collisions are not suppressed by the Fermi statistics at ultralow temperatures. In a dense atomic gas of density $n_{at} \sim 10^{13} - 10^{14}$ cm^{-3}, the collisional decay rate can be up to $\sim 10^4$ s^{-1} (with inelastic rate coefficient $K_{\text{inel}} \sim 0.5 - 1.0 \times 10^{-10}$ cm^{3}s^{-1} for Feshbach molecules (50; 51)). The STIRAP transfer must therefore be fast enough to avoid loosing molecules by inelastic decay. To alleviate this problem, we propose to start the STIRAP process directly from the scattering continuum without first forming Feshbach molecules. Using this approach with many STIRAP pulses and a fast repetition rate would also allow the conversion of nearly an entire atomic ensemble into ground state molecules, not only those atoms that were first transferred to a Feshbach molecular state.

Efficient adiabatic passage from the continuum requires laser pulses shorter than the coherence time of the continuum (27; 52; 53). The adiabaticity condition of STIRAP, $\Omega T \gg 1$, where T is the transfer time, therefore implies a large effective Rabi frequency Ω for the pulses. In addition, dipole matrix elements between the continuum and the bound state are usually small, and so the pump pulse that couples the continuum and the excited state would require a very high intensity, which proves impractical. Thus the previous STIRAP experiments (23), being restricted by the very short coherence time of the continuum, used a Feshbach molecular state as an initial state.

The small continuum-bound dipole matrix elements can be dramatically increased by photoassociating atoms in the vicinity of a Feshbach resonance. It has been shown, both theoretically and experimentally, that the photoassociation rate increases in the presence

of a Feshbach resonance by several orders of magnitude (54–57). This can be explained by considering that delocalized scattering states acquire some bound-state character due to admixture of a bound level associated with a closed channel, resulting in a large increase of the Franck-Condon factor between the initial scattering state and the final excited state. The recently proposed Feshbach Optimized Photoassociation (FOPA) technique (57) relies on this enhancement to directly reach deeply bound ground state vibrational levels from the scattering continuum. Consequently, photoassociation in the vicinity of a Feshbach resonance is expected to increase molecular formation rate up to 10^6 molecules/s (57).

Here we show that the approach used in FOPA can be combined with STIRAP for reducing the required pulse intensity. We predict highly efficient transfer of an entire atomic ensemble into the lowest rovibrational level in the molecular ground state. We note that a proposal, where the admixing of a short-range potential to a longer-range excited electronic potential, was recently suggested for improving a two-color pump-dump photoassociation scheme (58). The scattering continuum states have good overlap with the long-range potential, while the admixed short-range potential provides a good overlap with tightly bound vibrational levels of the ground electronic state, greatly improving the efficiency of photoassociation.

This section is organized as follows. In the next subsection, we derive a theoretical model of a combined atomic and molecular system. Fano theory is used to describe the interaction of a bound molecular state with the scattering continuum, represented as closed and open channel, respectively. The resulting continuum states are coupled by two laser fields to the vibrational target state in the ground state via the intermediate excited molecular electronic vibrational state. Next, we describe STIRAP-assisted conversion of a pair of colliding atoms into a deeply bound molecule. In subsection B, we present the results of numerical solutions of the model described in subsection A and in the Appendix B, using typical parameters of alkali dimers. We find optimal Rabi frequencies and profiles of STIRAP pulses. In subection C we average the pair-of-atoms STIRAP transfer efficiency over a thermal atomic ensemble, calculate a fraction of atoms that can be converted into molecules by one STIRAP sequence, and the number of pulses and overall time required to convert an entire atomic ensemble into molecules.

3.1 Model

We consider a three level system plus a continuum as shown in Figure 4, representing scattering states of two colliding atoms and bound states of a molecule. The ground level labeled $|1\rangle$ is the final product state to which a maximun of population must be transfered. Typically, this level will be the lowest vibrational level ($v'' = 0, J'' = 0$) of a ground molecular potential. This ground level is coupled to an excited bound level $|2\rangle$ of an excited molecular potential via a "Stokes" pulse depicted by the blue down-arrow in Figure 4. This level $|2\rangle$ is itself coupled via a pump pulse (red up-arrow) to an initial continuum of unbound scattering states $|\Psi_\epsilon\rangle$ of energies ϵ (shaded area in Figure 4). If we denote $C_1(t)$, $C_2(t)$ and $C(\epsilon, t)$ the time dependent amplitudes associated to the final, intermediate, and initial states $|1\rangle$, $|2\rangle$, and $|\Psi_\epsilon\rangle$, respectively, then the total wave function $|\Phi\rangle$ of the system is given by:

$$|\Phi\rangle = C_1(t)\,|1\rangle + C_2(t)\,|2\rangle + \int d\epsilon\; C(\epsilon, t)\,|\Psi_\epsilon\rangle\,. \tag{12}$$

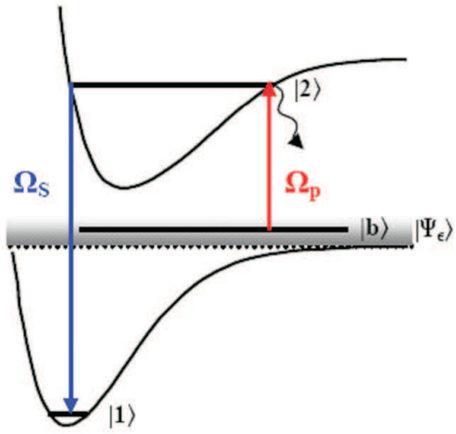

Fig. 4. Schematics: population from the initial state $|\Psi_\epsilon\rangle$ is transferred to a final target state $|1\rangle$ via an intermediate state $|2\rangle$. Both $|\Psi_\epsilon\rangle$ and $|1\rangle$ are coupled to $|2\rangle$ by a pump and a Stokes pulse, respectively labeled Ω_P and Ω_S. A bound level $|b\rangle$ corresponding to a closed channel can be imbedded in the continuum.

We assume that the levels associated with states $|1\rangle$ and $|2\rangle$ are well-isolated, and that there are no off-resonant laser couplings to other levels: this ensures the sufficient accuracy of the three-state model (see e.g. (23; 24; 59)).
No restriction applies to the definition of the continuum state $|\Psi_\epsilon\rangle$ as it can be associated to either a single-channel or a multi-channel scattering state. In this work, we consider the multi-channel case in which a bound level $|b\rangle$ associated to a closed channel is embedded in the continuum of scattering states $|\epsilon'\rangle$ of an open channel. When the energy of $|\epsilon'\rangle$ coincides with that of $|b\rangle$, a Feshbach resonance (14) occurs. These are common in binary collisions of alkali atoms due to hyperfine mixing and the tuning of the Zeeman interaction by an external magnetic field, hence the possibility to control interatomic interactions with a magnetic field. Following the Fano theory presented in Ref.(60), the scattering state $|\Psi_\epsilon\rangle$ can be expressed as:

$$|\Psi_\epsilon\rangle = a(\epsilon)\,|b\rangle + \int d\epsilon'\; b(\epsilon,\epsilon')\,|\epsilon'\rangle\ , \tag{13}$$

with

$$a(\epsilon) = \sqrt{\frac{2}{\pi\Gamma(\epsilon)}}\,\sin\Delta\ , \tag{14}$$

and

$$b(\epsilon,\epsilon') = \frac{1}{\pi}\sqrt{\frac{\Gamma(\epsilon')}{\Gamma(\epsilon)}}\,\frac{\sin\Delta}{\epsilon-\epsilon'} - \cos\Delta\;\delta(\epsilon-\epsilon')\ . \tag{15}$$

Here, $\Delta = -\arctan(\frac{\Gamma}{2(\epsilon-\epsilon_F)})$ is the phase shift due to the interaction between $|b\rangle$ and the scattering state $|\epsilon\rangle$ of the open channel. We assume $\Delta \in [-\pi/2, \pi/2]$. The width of the Feshbach resonance, $\Gamma = 2\pi|V(\epsilon)|^2$, is weakly dependent on the energy, while $V(\epsilon)$ is the interaction strength between the open and closed channels. The position of the resonance, $\epsilon_F = E_b + P\int \frac{|V(\epsilon')|^2 d\epsilon'}{\epsilon-\epsilon'}$, includes an interaction induced shift from the energy of the bound state E_b.

If we label E_i the energy of the state $|i\rangle$, the total Hamiltonian H is given by:

$$H = \sum_{i=1,2} E_i |i\rangle\langle i| + \int d\epsilon\ \epsilon |\Psi_\epsilon\rangle\langle\Psi_\epsilon| + V_{\text{light}}\ . \tag{16}$$

The light-matter interaction Hamiltonian V_{light} takes the form:

$$\begin{aligned} V_{\text{light}} = &-[\vec{\mu}_{21}|2\rangle\langle 1| + \text{H.c.}]\cdot\left(\vec{\mathcal{E}}_p + \vec{\mathcal{E}}_S + \text{c.c.}\right) \\ &-\int d\epsilon\ [\vec{\mu}_{2\Psi_\epsilon}|2\rangle\langle\Psi_\epsilon| + \text{H.c.}]\cdot\left(\vec{\mathcal{E}}_p + \vec{\mathcal{E}}_S + \text{c.c.}\right)\ , \end{aligned} \tag{17}$$

where $\vec{\mathcal{E}}_{p,S} = \hat{e}_{p,S}\mathcal{E}_{p,S}\exp(-i\omega_{p,S}t)$ are the pump and Stokes laser fields of polarization $\hat{e}_{p,S}$, respectively, while $\vec{\mu}_{21}$ and $\vec{\mu}_{2\Psi_\epsilon}$ are the dipole transition moments between the states $|2\rangle$ and $|1\rangle$, and $|2\rangle$ and $|\Psi_\epsilon\rangle$, respectively. In this form, the Hamiltonian already takes into account the mixing between the bound state of the closed channel and the scattering states of the open channel. The Schrödinger equation describing the STIRAP conversion of two atoms into a molecule gives:

$$i\hbar\frac{\partial C_1}{\partial t} = E_1\ C_1 - \vec{\mu}_{21}^{*}\cdot\vec{\mathcal{E}}_S^{*}\ C_2, \tag{18}$$

$$i\hbar\frac{\partial C_2}{\partial t} = E_2\ C_2 - \vec{\mu}_{21}\cdot\vec{\mathcal{E}}_S\ C_1 \tag{19}$$

$$-\int_{\epsilon_{th}}^{\infty} d\epsilon\ \vec{\mu}_{2\Psi_\epsilon}\cdot\vec{\mathcal{E}}_p\ C(\epsilon,t),$$

$$i\hbar\frac{\partial C(\epsilon,t)}{\partial t} = \epsilon\ C(\epsilon,t) - \vec{\mu}_{2\Psi_\epsilon}^{*}\cdot\vec{\mathcal{E}}_p^{*}\ C_2. \tag{20}$$

For simplicity, we set the origin of the energy to be the position of the ground state $|1\rangle$, and use the rotating wave approximation with $C_1 = c_1$, $C_2 = c_2 e^{-i\omega_S t}$, and $C(\epsilon,t) = c(\epsilon,t)e^{-i(\omega_S-\omega_P)t}$. Eqs.(18)-(20) then become:

$$i\frac{\partial c_1}{\partial t} = -\Omega_S c_2, \tag{21}$$

$$i\frac{\partial c_2}{\partial t} = \delta c_2 - \Omega_S c_1 - \int_{\epsilon_{\text{th}}}^{\infty} d\epsilon\ \Omega_\epsilon c(\epsilon,t), \tag{22}$$

$$i\frac{\partial c(\epsilon,t)}{\partial t} = \Delta_\epsilon c(\epsilon,t) - \Omega_\epsilon^{*} c_2, \tag{23}$$

where $\delta = E_2/\hbar - \omega_S$, $\Delta_\epsilon = \epsilon/\hbar - (\omega_S - \omega_p)$, and ϵ_{th} is the dissociation energy of the ground electronic potential with respect to the state $|1\rangle$. The Rabi frequencies of the fields are $\Omega_S = \vec{\mu}_{21}\cdot\hat{e}_S\mathcal{E}_S/\hbar$ (assumed real), $\Omega_\epsilon = \vec{\mu}_{2\Psi_\epsilon}\cdot\hat{e}_p\mathcal{E}_p/\hbar$.

The previous system of three equations can be reduced into a two-equation system by eliminating the continuum amplitude $c(\epsilon,t)$ in Eq.(23). Introducing a solution in the form of $c(\epsilon,t) = s(\epsilon,t)\exp(-i\Delta_\epsilon t)$ into Eq.(23), we get

$$s = i\int_0^t dt'\ \Omega_\epsilon^{*}(t')c_2(t')e^{i\Delta_\epsilon t'} + s(\epsilon,t=0), \tag{24}$$

where $t = 0$ is some moment before the collision of the two atoms. The resulting continuum amplitude is

$$c(\epsilon, t) = i \int_0^t dt' \; \Omega_\epsilon^*(t') c_2(t') e^{i\Delta_\epsilon (t'-t)} + s(\epsilon, t=0) e^{-i\Delta_\epsilon t}. \tag{25}$$

Inserting this result into Eq. (22), we obtain a final system of equations for the amplitudes of the bound states:

$$i\frac{\partial c_1}{\partial t} = -\Omega_S c_2 \,, \tag{26}$$

$$\begin{aligned} i\frac{\partial c_2}{\partial t} &= (\delta - i\gamma) c_2 - \Omega_S c_1 - \int_{\epsilon_{\rm th}}^{\infty} d\epsilon \; \Omega_\epsilon(t) s(\epsilon, t=0) e^{-i\Delta_\epsilon t} \\ &\quad + i \int_{\epsilon_{\rm th}}^{\infty} d\epsilon \; \Omega_\epsilon(t) \int_0^t dt' \; \Omega_\epsilon(t')^* c_2(t') e^{i\Delta_\epsilon (t'-t)} \\ &\equiv (\delta - i\gamma) c_2 - \Omega_S c_1 - S + T \,, \end{aligned} \tag{27}$$

where we introduced a spontaneous decay term γc_2 in Eq.(27).
The third term of Eq.(27), labelled S, corresponds to the source function, wheareas the last term, labelled T, corresponds to the "back-stimulation" term (or back-conversion) which accounts for the transfer of the bound molecules back into the continuum. The initial amplitude of the continuum wave function $s(\epsilon, t = 0)$ appearing in the source term has been discussed in various contributions (27; 52; 53). A Gaussian wavepacket provides the most classical description of a two-atom collision characterized by a minimal uncertainty relation between the energy bandwidth δ_ϵ of the wavepacket and the duration of the collision:

$$s(\epsilon, t=0) = \frac{1}{(\pi \delta_\epsilon^2)^{1/4}} e^{-\frac{(\epsilon-\epsilon_0)^2}{2\delta_\epsilon^2} + \frac{i}{\hbar}(\epsilon-\epsilon_0) t_0}, \tag{28}$$

where t_0 is the moment of the collision and ϵ_0 is the central energy of the wavepacket.
Futhermore, the Rabi frequency of the field coupling continuum states $|\Psi_\epsilon\rangle$ to the state $|2\rangle$ is given by (60)

$$\Omega_\epsilon = \frac{\vec{\mu}_{2\epsilon} \cdot \hat{e}_p \mathcal{E}_p}{\hbar} \frac{q\Gamma/2 + \epsilon - \epsilon_F}{\sqrt{(\Gamma/2)^2 + (\epsilon - \epsilon_F)^2}} \mathrm{sgn}(\epsilon - \epsilon_F), \tag{29}$$

where $\vec{\mu}_{2\epsilon}$ is the dipole matrix element between an unperturbed scattering state $|\epsilon\rangle$ and the state $|2\rangle$, and q is the Fano parameter, expressed as:

$$q = \frac{(\vec{\mu}_{2b} \cdot \hat{e}_p) + P \int \frac{V(\epsilon')(\vec{\mu}_{2\epsilon'} \cdot \hat{e}_p) d\epsilon'}{\epsilon - \epsilon'}}{\pi V^*(\epsilon)(\vec{\mu}_{2\epsilon} \cdot \hat{e}_p)}, \tag{30}$$

where $\hat{e}_p$ is the polarization vector of the pump field, and $\vec{\mu}_{2b}$ is the dipole matrix element between bound states $|2\rangle$ and $|b\rangle$. The q factor is essentially the ratio of the dipole matrix elements from the state $|2\rangle$ to the bound state $|b\rangle$ (modified by the continuum) and to an unperturbed continuum state $|\epsilon\rangle$. This factor can be made much larger than unity, and as will be shown below, the total dipole matrix element from the continuum can be enhanced by this factor in the presence of the resonance. The magnitude of q can be controlled by the choice of the vibrational state $|2\rangle$. Selecting a tightly bound excited vibrational state will increase the

bound-bound and decrease the continuum-bound dipole matrix elements, resulting in larger q, whereas choosing a highly excited state close to a dissociation threshold will decrease q.
Using the expressions given in Eqs.(28), (29), and (30) for the initial amplitude of the continuum wave function, the Rabi frequency between the continuum state $|\Psi_\epsilon\rangle$ and the excited bound state $|2\rangle$, and the Fano parameter, respectively, we obtain the following complete expression for the source term:

$$S = S_0 \int_{\epsilon_{\rm th}}^{\infty} d\epsilon \; g(q,\epsilon) \; \mathrm{sgn}(\epsilon - \epsilon_F) e^{-\frac{(\epsilon-\epsilon_0)^2}{2\delta_\epsilon^2} + \frac{i(\epsilon-\epsilon_0)t_0}{\hbar}} e^{-i\Delta_\epsilon t}, \tag{31}$$

with $S_0 = \vec{\mu}_{2\epsilon} \cdot \hat{e}_p \mathcal{E}_p / \hbar (\pi \delta_\epsilon)^{1/4}$, and where the function $g(q,\epsilon)$ is defined as

$$g(q,\epsilon) \equiv \frac{q + \frac{2}{\Gamma}(\epsilon - \epsilon_F)}{\sqrt{1 + \frac{4}{\Gamma^2}(\epsilon - \epsilon_F)^2}}. \tag{32}$$

We assume that the unperturbed continuum is structureless and that the corresponding Rabi frequency $\vec{\mu}_{2\epsilon} \cdot \hat{e}_p \mathcal{E}_p / \hbar$ depends only weakly on the energy. We also extend $\epsilon_{\rm th}$ to $-\infty$ to have the initial continuum wavefunction normalized to unity[1]: $\int_{-\infty}^{\infty} d\epsilon |C(\epsilon)|^2 = 1$.
We can as well obtain a complete expression for the back-stimulation term T. We have:

$$T = \left| \frac{\vec{\mu}_{2\epsilon} \hat{e}_p}{\hbar} \right|^2 \mathcal{E}_p(t) \int_{\epsilon_{th}}^{\infty} d\epsilon \; g^2(q,\epsilon) \int_0^t dt' \; c_2(t') \mathcal{E}_p(t') e^{i\Delta_\epsilon (t'-t)}. \tag{33}$$

Extending the lower integration limit[2] allows for an analytical solution for the integrals over energy and time, leading to the following expression for the back-stimulation term:

$$T = \left| \frac{\vec{\mu}_{2\epsilon} \hat{e}_p}{\hbar} \right|^2 \left[\pi \hbar \mathcal{E}_p^2(t) c_2(t) + \frac{\pi \Gamma}{2} (q-i)^2 \mathcal{E}_p(t) \right.$$
$$\left. \times \int_0^t dt' \; c_2(t') \mathcal{E}_p(t') e^{[\Gamma/2\hbar + i(\epsilon_F/\hbar - \omega_S + \omega_p)](t'-t)} \right]. \tag{34}$$

3.2 Results of STIRAP transfer for a pair of atoms

In this subsection, we consider two different cases: first, when $\Gamma \gg \delta_\epsilon$, *i.e.*, when the width Γ of the Feshbach resonance is much larger than the thermal energy spread δ_ϵ of the colliding atoms, and second when $\Gamma \ll \delta_\epsilon$. By considering these two limiting cases of broad and narrow

[1] Extension of $\epsilon_{\rm th}$ to $-\infty$ in the source term (31) can be justified by the sharp reduction of the Gaussian term $\exp(-(\epsilon_{\rm th} - \epsilon_0)^2/2\delta_\epsilon^2)$ for $\epsilon_0 - \epsilon_{th} > \delta_\epsilon$. For ϵ_0 close to $\epsilon_{\rm th}$, this approximation is less accurate, but as will be shown in Section IV, these low energies give negligible contribution to transfer efficiency averaged over an atomic ensemble due to their small weight in the Maxwell-Boltzmann distribution.

[2] The extension of the lower integration limit to $-\infty$ in the back-stimulation term (33) can be explained by the following argument. For an optimal transfer the duration of laser pulses has to be of the order of the coherence time of the populated continuum, given by $1/\delta_\epsilon$. The period of the exponent $\exp(i\Delta_\epsilon(t'-t))$ on the other hand is given by $2\pi/\Delta_\epsilon$. The integral over time therefore quickly goes to zero if this period is smaller then the duration of pulses. As a result, the time integral is non-zero only for energies $|\Delta_\epsilon| = |\epsilon/\hbar - (\omega_S - \omega_p)| < \delta_\epsilon$. In the case of the pump laser resonant with the center of the thermal distribution $|\epsilon_{\rm th} - (\omega_S - \omega_p)| \sim \delta_\epsilon$, and the extension of the energy integration to $-\infty$ is well-justified.

Reso-nance	δ_ϵ μK	Γ μK	Ω_S^0 10^8 s^{-1}	I_S W/cm^2	I_p W/cm^2	T_S μs	T_p μs	τ_S μs	τ_p μs
None	10	—	0.72	62	4×10^5	1.5	3	0.75	1.0
Broad	10	1000	0.74	65	4000	1.4	3.4	0.65	1.0
Narrow	100	1	2.24	600	400	0.157	0.3	0.1	0.207

Table 2. Parameters of the Stokes and pump photoassociating pulses providing optimal population transfer for a pair of atoms shown in Fig.5. We use $q = 10$, $\gamma = 10^8$ s^{-1}, and $\mu_{2b} = \mu_{21} = 0.1$ D. Rabi frequencies are modeled by Gaussians $\Omega_{S,p} = \Omega^0_{S,p} \exp\left(-(t - t_0 \pm \tau_{S,p})\right)/T^2_{S,p}$, where $\pm$ refers to the Stokes and pump pulse, respectively.

resonances, more practical expressions for both the source term S and the back stimulation term T can be found. The derivation of the final system of equations used in numerical solutions is given in Appendix B. Here, we describe the solutions of these systems for both broad and narrow resonances.

We note that during the transfer an initial incoherent mixture of atomic scattering states is converted into a pure internal state, which seems to decrease the entropy of the system. However, the entropy is transferred to the center-of-mass motion of the created molecules, which can lead to a slight translational heating of the sample.

Using Eqs.(A3)-(A4) and (A7)-(A8) with the parameters listed in Table 2 for a broad ($\Gamma = 1$ mK) and a narrow ($\Gamma = 1$ μK) Feshbach resonance, we obtain the results for the STIRAP transfer of an atom pair, depicted in Fig. 5. Here the left column corresponds to the broad resonance, and the right column to the narrow resonance. The top row shows the variation of the Rabi frequencies over the time period required for the population transfer along with population in the intermediate state $|2\rangle$ (middle row) and final state $|1\rangle$ (bottom row).

For the broad case, we considered a Feshbach resonance with a width $\Gamma = 1$ mK (typical for broad resonances), and a thermal atomic ensemble with an energy bandwidth $\delta_\epsilon = 10$ μK. We see that the transfer efficiency can reach $\sim$ 97% of the continuum state into the target state $|1\rangle$ (see Fig. 5 c). The parameters of the Gaussian laser pulses used (optimized Rabi frequencies, durations and delays of laser pulses) are given in Table 2: the peak intensities of the Stokes and pump fields were calculated from Rabi frequencies as $I_S = c\mathcal{E}_S^2/8\pi = c(\Omega_S^0\hbar)^2/8\pi\mu_{21}^2$ and $I_p = c\mathcal{E}_p^2/8\pi = c(\Omega_p^0)^2\delta_\epsilon/32\pi^{3/2}\mu_{2\epsilon}^2$, where we use Eq.(30) to estimate the continuum-bound dipole matrix element $\mu_{2\epsilon} \approx \mu_{2b}/q\pi V(\epsilon) = \sqrt{2}\mu_{2b}/q\sqrt{\pi\Gamma}$, resulting in $I_p = q^2 c(\Omega_p^0)^2\delta_\varepsilon\Gamma/64\sqrt{\pi}\mu_{2b}^2$.

When comparing the results for a broad resonance to that of the unperturbed continuum (*i.e.*, far from the resonance), we find that the source term S is enhanced by the factor $g(q, \epsilon_0)$ (see Eq. (38) in Appendix B):

$$g(q,\epsilon_0) = \frac{q + \frac{2}{\Gamma}(\epsilon_0 - \epsilon_F)}{\sqrt{1 + \frac{4}{\Gamma^2}(\epsilon_0 - \epsilon_F)^2}}. \tag{35}$$

This factor has a maximum at $2(\epsilon_0 - \epsilon_F)/\Gamma = 1/q$, with the corresponding maximum value $\sqrt{1+q^2} \approx q$ for $q \gg 1$: hence, the source amplitude is enhanced q times. In this limit, all populated continuum states experience the same transition dipole matrix element enhancement factor to the state $|2\rangle$, so that the system essentially reduces to the case of a flat

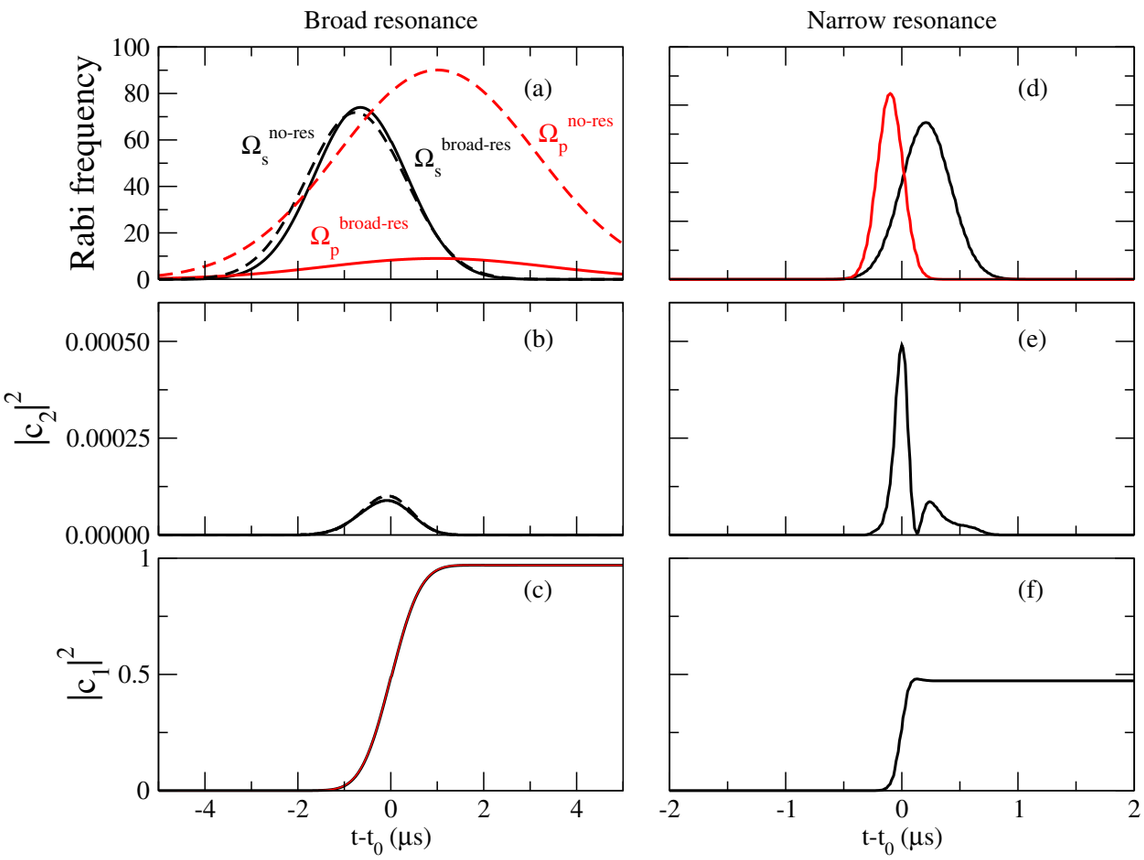

Fig. 5. Time-dependence of the Stokes and pump pulses (top row) and population in state $|2\rangle$ (middle row) and target state $|1\rangle$ (bottom row) for the STIRAP transfer of a pair of atoms within the center of the thermal distribution. The left column is for a broad Feshbach resonance, while the right column is for a narrow resonance (see Table 2 for values of parameters used). The dashed blue lines in the left column are the results obtained without resonance, when the parameters are adjusted to obtain the same overall transfer efficiency as for the broad resonance. The Stokes Rabi frequency is in units of 10^6 s^{-1}, while the pump Rabi frequency is in dimensionless units $(16\pi/\delta_\epsilon)^{1/4}\,\vec{\mu}_{2\epsilon}\hat{e}_p\mathcal{E}_p$ in the broad resonance limit and $(2\pi/\Gamma)^{1/2}\,\vec{\mu}_{2\epsilon}\hat{e}_p\mathcal{E}_p$ in the narrow resonance limit. Note that the scale for the Rabi frequencies in the narrow resonance case is 40 times the scale for the broad resonance, and the magnitude of the pump Rabi frequency is enlarged 10 times for better visibility.

continuum with an uniformly enhanced transition dipole matrix element. One thus expects that in this limit, the adiabatic passage should be efficient, requiring less pump laser intensity when compared to the unperturbed (*i.e.* without resonance) scattering continuum. This is clearly demonstrated in Fig. 5 (left column, dashed lines): to reach the same $\sim$ 97% transfer efficiency achieved with the broad resonance, a very large pump laser intensity ($\sim$ 100 times larger) is required if there is no resonance in the continuum (Fig. 5 a), while the Stokes laser intensity is basically the same. Considering the intensity used in this particular example, this would lead to intensities in the range of 5×10^5 W/cm^2, making STIRAP from the continuum technically impossible to achieve without a resonance. This is consistent with the analysis of photoassociative adiabatic passage from an unstructured continuum (27), and the above

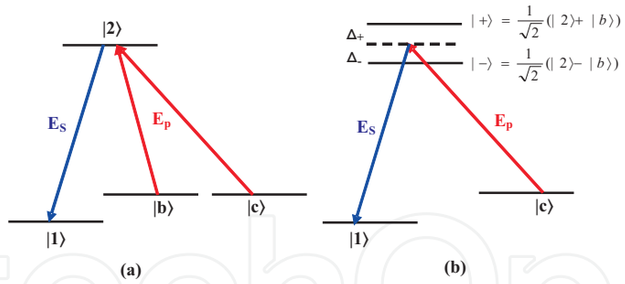

Fig. 6. Illustration of the reduction of STIRAP transfer efficiency due to destructive quantum interference for a narrow resonance: (a) a simplified level scheme where the scattering continuum is modeled by a single state $|c\rangle$ and the interaction between the continuum and the Feshbach state $|b\rangle$ is neglected; (b) an equivalent scheme, where the strong coupling between the Feshbach state $|b\rangle$ and the excited state $|c\rangle$ by the pump field forms "dressed" states $|\pm\rangle$. We have the Rabi frequency $\Omega_{2c} = \Omega_{+c}^2/\Delta_+ + \Omega_{-c}^2/\Delta_- = 0$, since $\Omega_{+c} = \Omega_{-c}$ and $\Delta_+ = -\Delta_-$.

prediction that in the presence of a wide resonance the required pump laser intensity is reduced by a factor of $\sim 1/q^2$.

Results of adiabatic passage for a pair of atoms in a narrow resonance limit are shown in Fig. 5 (right column). We considered typical values for a narrow resonance width $\Gamma = 1$ μK and the ensemble energy bandwidth $\delta_\epsilon = 100$ μK. Again, we give the parameters providing the optimal transfer in Table 2. In this limit, the transfer efficiency is lower: in the specific case analyzed here, it does not exceed 47%. The reason for this lower efficiency compared to a wide resonance is the destructive quantum interference which leads to electromagnetically induced transparency (61) in the transition from the continuum to the excited state. It can be explained using the following argument (see Fig. 6). The limit of a narrow Feshbach resonance corresponds to a weak coupling between the bound Feshbach state and the scattering continuum, and thus can be neglected in this simplified explanation. The system then can be viewed as consisting of bound and continuum states $|b\rangle$ and $|c\rangle$ having the same energy, which are coupled by the pump field to a molecular state $|2\rangle$, itself coupled to the state $|1\rangle$ by the Stokes field. Assuming that initially all the population is in the state $|c\rangle$, due to the small interaction strength between $|b\rangle$ and $|c\rangle$, we can eliminate the state $|b\rangle$, taking into account its coupling to $|2\rangle$ by the pump laser as the formation of "dressed" states $|\pm\rangle = (|2\rangle \pm |b\rangle)/\sqrt{2}$. If the dipole matrix element of the $|b\rangle \to |2\rangle$ transition is much larger than that of the $|c\rangle \to |2\rangle$ transition, the detuning of the "dressed" states satisfies $|\Delta_\pm| = \Omega_p^{2b} \gg \Omega_p^{2c}$, Ω_S. As a result, the one-photon coupling of $|c\rangle$ to the excited state, as well as two-photon coupling to $|1\rangle$ vanishes, preventing the adiabatic transfer. This mechanism is similar to the Fano interference effect, the difference is that the continuum is initially populated. One can therefore view it as an inverse Fano effect. The effective dipole matrix element of the $|c\rangle \to |2\rangle$ transition is $\mu_{2c} \sim \mu_{2b}/q\sqrt{\xi}$. In the case we analyzed, $q = 10$, $\xi = \Gamma/\sqrt{2}\delta_\epsilon = 0.01$, and $\mu_{2c} \approx \mu_{2b}$, which gives $\sim 50\%$ transfer efficiency.

The transfer efficiency increases if the Feshbach state is far detuned from the populated continuum. Our calculations show that for a Feshbach state detuning $\epsilon_F/\hbar - (\omega_S - \omega_p) \gg |\Omega_{2b}|^2/\gamma$, the transfer efficiency reaches 70% using the laser pulse parameters in Table 2. We note that the smaller intensity of the pump pulse used for the narrow resonance, as compared to the broad resonance, is due to the fact that we used the same $q = 10$ and assumed $\mu_{2b} = 0.1$

Reso-nance	δ_ϵ μK	Γ μK	Ω_S^0 10^8 s^{-1}	I_S W/cm^2	I_p W/cm^2	T_S μs	T_p μs	τ_S μs	τ_p μs
None	10	—	0.50	30	1.7×10^5	1.5	3.3	0.75	1.3
Broad	10	1000	0.60	40	2500	1.3	3.2	0.7	1.25
Narrow	100	1	2.24	600	400	0.157	0.3	0.1	0.207

Table 3. Parameters of the Stokes and pump photoassociating pulses providing optimal population transfer shown in Fig.7 for averaging over a Maxwell-Boltzmann distribution of energies. We use $q = 10$, $\gamma = 10^8$ s^{-1}, and $\mu_{2b} = \mu_{21} = 0.1$ D (1 D=10^{-18} esu cm = 0.3934 ea_0).

D for both resonances. From the definition of q, it means that the continuum-bound dipole matrix element $\mu_{2\varepsilon}$ is higher in the narrow than in the broad resonance we considered. This explains the smaller resulting pump pulse intensity. The overall conclusion for a narrow resonance is that, as opposed to a broad resonance, the presence of the Feshbach resonance prevents one from realizing high transfer efficiencies. It should be noted, however, that the destructive quantum interference effect is based on negligible interaction between the Feshbach and continuum states during the transfer time, since $T < \delta_\varepsilon^{-1} \ll \Gamma^{-1}$. This argument shows that already for $\Gamma \geq \delta_\epsilon$, there is enough interaction to neutralize the effect of destructive interference. Therefore, we expect that the broad resonance limit can be extended down to $\Gamma \sim \delta_\epsilon$, making it applicable to a wide variety of atomic species.

3.3 Conversion of atomic ensembles into ground state molecules

The results of Fig. 5 were obtained for a pair of atoms having a specific mean collision energy $\epsilon_0 = \hbar(\omega_S - \omega_p)$. Such a situation could be realized in very tight traps, *e.g.*, in tight optical lattices. For a system with a wider energy distribution, one would like to find an ensemble averaged transfer efficiency, and thus one needs to calculate the transfer probability $P(\epsilon_0) = |c_1|^2$ for all central wavepacket energies ϵ_0 within the thermal spread of energies, and perform the averaging as

$$P_{\rm avg} = \frac{2}{\sqrt{\pi}(k_B T)^{3/2}} \int_0^\infty e^{-\epsilon_0/k_B T} \sqrt{\epsilon_0} P(\epsilon_0) d\epsilon_0, \tag{36}$$

where we assume a Maxwell-Boltzmann energy distribution, the pump laser resonant with the center of the distribution at $\langle\epsilon\rangle = 3/2 k_B T$, and set the bandwidth of the distribution at $\delta_\epsilon = \sqrt{\langle(\Delta\epsilon)^2\rangle} = \sqrt{3/2} k_B T$. The results are shown in Fig.7: while the maximum transfer efficiency in the broad resonance case is $\sim 70\%$, it can be achieved with lower laser intensities than in the case of a pair of atoms of Fig.5.

Given the adiabatic photoassociation probability $P(\epsilon)$ for two colliding atoms with relative energy ϵ, we can calculate the number of atoms photoassociated during the time overlap τ of the Stokes and pump pulses. During this time, the atom with the energy $\epsilon = \mu v^2/2$, where μ is the reduced mass, will collide with atoms in the volume $\pi b^2 v\tau$, where πb^2 is the collision cross-section. The impact parameter for the collision corresponding to a partial wave with angular momentum ℓ is $b = (\ell + 1/2)\hbar/p = (\ell + 1/2)\hbar/\sqrt{2\mu\epsilon}$. The number of collisions that atoms with a relative energy in the interval $(\epsilon, \epsilon + d\epsilon)$ will experience during the transfer time is therefore $N(\epsilon)d\epsilon = \pi b^2 v\tau\rho(\epsilon)d\epsilon$, where $\rho(\epsilon) = 2\rho \exp(-\epsilon/k_B T)\sqrt{\epsilon}/\sqrt{\pi}(k_B T)^{3/2}$ is the spectral density of the atoms (ρ is the density of the sample). Finally, $\ell = 0$ for ultracold s-wave collisions, and the fraction of atoms in the energy interval $(\epsilon, \epsilon + d\epsilon)$ photoassociated

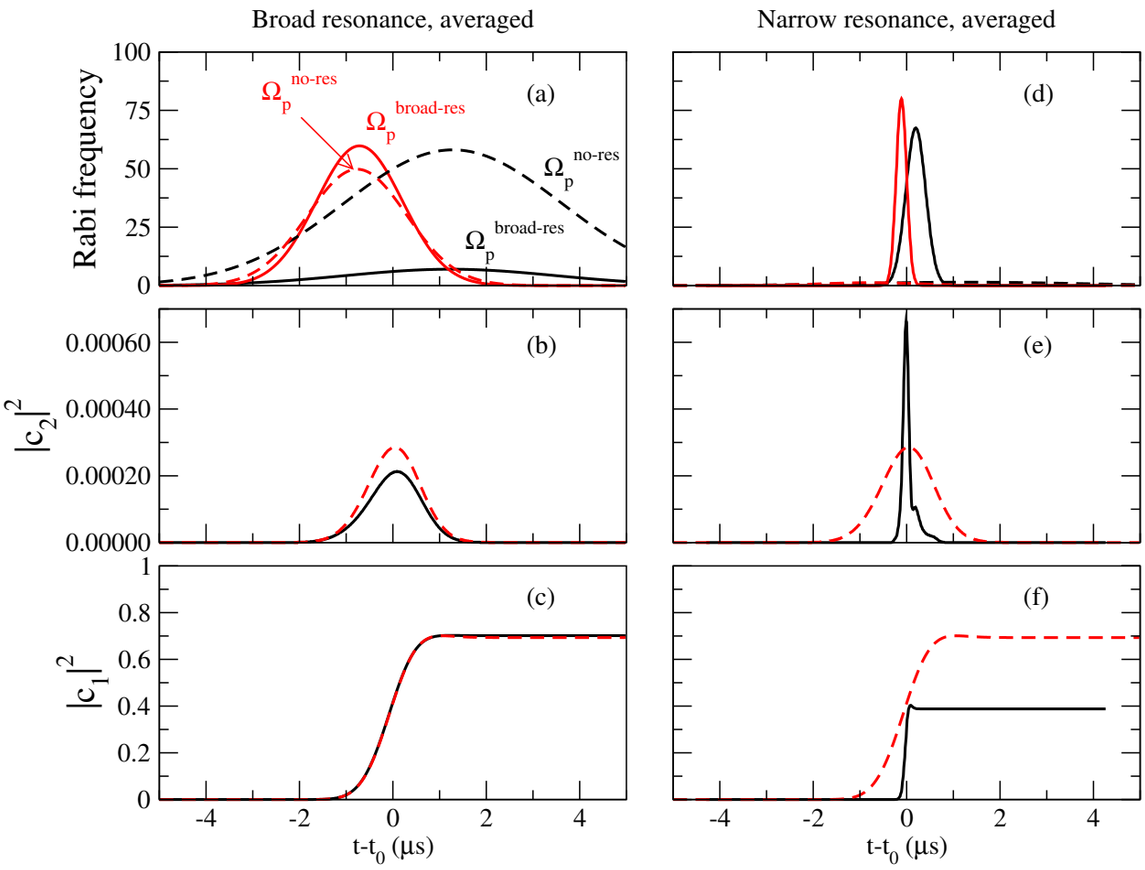

Fig. 7. Same as Fig. 5, but for the energy averaged transfer. The parameters are listed in Table 3.

by the two pulses is $f(\epsilon) = P(\epsilon)N(\epsilon)$, or

$$f(\epsilon) = \frac{\sqrt{2\pi}\hbar^2}{4(\mu k_B T)^{3/2}} \tau \rho P(\epsilon) \exp\left(-\epsilon/k_B T\right). \tag{37}$$

The total fraction of atoms photoassociated by a pair of pulses is $f = \int_0^\infty d\epsilon \; f(\epsilon) \approx P_{\rm avg}\rho\sqrt{2\pi}\tau\hbar^2/4\mu^{3/2}\sqrt{k_B T}$, where we assumed that $P(\epsilon)$ does not significantly vary within the ensemble, and approximated it by the averaged value $P_{\rm avg}$. Considering as an example ^{6}Li atoms at $T = 100$ μK with an atomic density $\rho = 10^{12}$ cm^{-3}, an overlap time $\tau \sim 1$ μs, and assuming $P_{\rm avg} = 0.7$, the fraction of atoms photoassociated by the Stokes and pump pulses is $f \sim 2.5 \times 10^{-4}$: for heavier atoms $f \sim 10^{-6} - 10^{-5}$. It will therefore require $\sim 10^4 - 10^6$ pairs of pulses to convert an entire atomic ensemble into deeply bound molecular levels.

As was shown in (62), in the limit of a narrow resonance longer pulses with durations $T_S, T_p \sim 1/\Gamma$ can be used. The reason is that population gets "trapped" in the bound state $|b\rangle$ for a time $\sim 1/\Gamma$ (it can be seen from the expression for the narrow resonance source function A.6), and as a result coherent transfer is still possible. The fraction of atoms associated per pulse pair in this case is comparable to the case of a wide resonance, since the smaller transfer efficiency $P(\epsilon)$ is compensated by a larger pulse overlap τ. The long pulse duration results in

its narrow bandwidth $\sim \Gamma$, much smaller than the thermal ensemble energy δ_ϵ. Conversion efficiency per pulse pair in this case might be increased by simultaneously chirping the Feshbach resonance energy and the pump pulse frequency, i.e. by tuning ϵ_F and ω_P in time keeping the two-photon resonance condition $\epsilon_F = \omega_S - \omega_p$ satisfied.

While only a small fraction of atoms can be transferred to $|1\rangle$ by a pair of STIRAP pulses, a train of pulse pairs can be applied to photoassociate the entire atomic ensemble. To prevent excitation of molecules in $|1\rangle$ back to the continuum by subsequent pulses, they have to be removed before the next pair of pulses is applied. This could be realized by applying, after each pair of Stokes and pump pulses, a relatively long pulse resonant to a transition from $|1\rangle$ to some other vibrational level in the excited electronic potential which decays spontaneously to a deep vibrational state in the ground electronic potential. This long pulse would optically pump molecules out of the state $|1\rangle$ to deeper vibrational states in the ground electronic potential. It therefore has to be longer than the spontaneous decay time of the excited state. The excited state has to be chosen carefully so that it does not decay back into the scattering continuum. This would empty the $|1\rangle$ state and deposit molecules into ground potential vibrational states according to Franck-Condon factors before the next pair of pulses arrives. Finally, after all atoms have been converted into molecules the recently demonstrated optical pumping for molecules method (20) can be applied, which would transfer molecules from all populated vibrational states into the ground level $v = 0$.

The optimal strategy is to actually choose an excited state that decays mostly to the $v = 0$ level. This would allow one to avoid storing molecules in unstable vibrational states and using the optical pumping method. If such a state cannot be directly reached from $|1\rangle$, a four-photon STIRAP transfer can be applied (30), which provides efficient transfer to deeply bound molecular states. It allows one to choose the final state $|1\rangle$, from which the excited state decaying predominantly to $v = 0$ can be easily reached. In this case rotational selectivity can also be preserved, since only $v = 0, J = 0$ and $v = 0, J = 2$ states will be populated.

The total time required to photoassociate the whole atomic ensemble and transfer it to the $v = 0$ level can be estimated as follows. As the numerical results show, the adiabatic passage requires ~ 5 μs, the follow-up pulse emptying state $|1\rangle$ can have a ~ 100 ns duration, if the excited state lifetime is tens of ns, resulting in the whole sequence ~ 6 μs. Then the train of $10^4 - 10^6$ pulse pairs will take $\sim 0.1 - 10$ s. The final step, optical pumping to the $v = 0$ level, requires $\sim$ hundred μs, so the overall formation time is $\sim 0.1 - 10$ s. Given an illuminated volume $\sim 10^{-2} - 10^{-3}$ mm^3 and an atomic density $\rho \sim 10^{12}$ cm^{-3}, the resulting production rate is expected to be $10^5 - 10^8$ molecules/s. This compares well with recent experiments on STIRAP production of ground state KRb molecules starting from the Feshbach bound state, where $\sim 3 \times 10^4$ ground state molecules are produced during the entire cycle, including creation of Feshbach molecules, taking $\sim 10 - 30$ s (23).

Alternatively, back-stimulation of formed molecules into the continuum by subsequent STIRAP pulses can be avoided by placing them in a moving optical lattice, holding molecules but not atoms (27). Another way to avoid back-stimulation, applicable to polar molecules, is to overlap the atomic trap with a gradient of a DC electric field. It will leave dipoleless atoms unaffected, while shifting molecules out of STIRAP laser beams.

To summarize, combining both photoassociation and coherent optical transfer to rovibrational levels of the ground electronic molecular potential can allow one to convert an entire atomic ensemble into deeply bound molecular states, and to produce an ultracold molecular gas with high phase-space density. Photoassociative adiabatic passage in a thermal ultracold

atomic gas can be greatly facilitated by a Feshbach resonance. The presence of a bound state imbedded in and resonant with scattering continuum states strongly enhances the continuum-bound transition dipole matrix element to an excited electronic state, thus requiring less laser intensity for efficient transfer. In the limit of a wide resonance, when compared to the thermal spread of collision energies, the dipole matrix element is enhanced by the Fano parameter q. By choosing a tightly bound excited vibrational state, q can be made much larger than unity, resulting in the intensity of the pump pulse required for efficient adiabatic passage to be $\sim 1/q^2$ times smaller than in the absence of the resonance. Numeical modeling of the adiabatic passage using typical parameters of alkali dimers shows that intensities of the pump pulse, coupling the continuum to an excited state, of kW/cm^2 are sufficient for optimal transfer, which is ~ 100 times smaller than without resonance. Optimal pulse durations are several μs, resulting in energies per pulse ~ 10 μJ for a focus area of 1 mm^2.

If the Feshbach resonance is narrow compared to the thermal energy spread of colliding atoms, adiabatic passage is hindered by destructive quantum interference. The reason is that electromagnetically induced transparency significantly reduces the transition dipole matrix element from the scattering continuum to an excited state in the presence of the bound Feshbach state. In the narrow resonance limit, photoassociative adiabatic passage is therefore more efficient if the resonance is far-detuned.

Due to low atomic collision rates at ultracold temperatures, only a small fraction of atoms can be converted into molecules by a pair of photoassociative pulses. To convert an entire atomic ensemble, a train of pulse pairs can be applied. We estimate that $10^4 - 10^6$ pulse pairs will associate an atomic gas of alkali dimers with a density 10^{12} cm^{-3} in an illuminated volume of $10^{-2} - 10^{-3}$ mm^3 in $0.1 - 10$ s, resulting in extremely high production rates of $10^5 - 10^8$ molecules/s. High transfer efficiencies combined with low intensities of adiabatic photoassociative pulses also make the broad resonance limit attractive for quantum computation. For example, a scheme proposed in (63) can be realized, where qubit states are encoded into a scattering and a bound molecular states of polar molecules. To perform one and two-qubit operations, this scheme requires a high degree of control over the system, which our model readily offers.

Finally, marrying FOPA and STIRAP is a very promising avenue to produce large amounts of molecules, for a variety of molecular species. In fact, although we described here examples based on magnetically induced Feshbach resonances, such resonances are extremely common, and can be induced by several interactions, such as external electric fields or optical fields. Even in the absence of hyperfine interactions, other interactions can provide the necessary coupling, such as in the case of the magnetic dipole-dipole interaction in ^{52}Cr (64; 65).

4. Conclusions

Precise control over internal and external degrees of freedom of molecules will open the way for new fundamental studies and applications in physics and chemistry. As has been clearly seen with atoms in the recent decades, well-controlled laser fields offer an exquisite control tool over atomic internal and external states, including laser cooling and trapping, coherent manipulation of atomic quantum states and in particular various techniques used for quantum information applications, atomic spectroscopy. Recent years have witnessed mastering of single atom manipulation in individual traps, including optical dipole traps and

atom chips, and optical lattices, with most manipulation techniques relying on laser fields. There is a great incentive in the atomic and molecular optics community to extend the precise control techniques developed for atoms to molecules. We have outlined in this chapter some experimentally relatively simple laser pulse techniques that can accomplish this task.
A prerequisite for many of the new studies is a high phase space density molecular sample in a stable internal state, specifically in the ground rovibrational state and preferably in the lowest hyperfine sublevel. We have in particular discussed two examples of coherent laser control of molecular states, multistate chainwise STIRAP and photoassociatice adiabatic passage near Feshbach resonance, which provide efficient transfer of molecules to the ground rovibrational state. In chainwise STIRAP the transfer is based on a generalized dark state, which is a superposition of all ground vibrational levels involved in the process. Selecting a special time order of the laser pulses coupling vibrational states and optimizing durations and intensities transfer efficiencies $> 90\%$ are predicted even in the presence of fast collisional decay of intermediate vibrational states. This technique has recently been applied to transfer Cs_2 Feshbach molecules to the ground rovibrational state with 55% efficiency, limited by technical issues. Additionally, we outlined how the step from the atomic scattering continuum to the ground rovibrational molecular state can be done in one coordinated step. In the presence of a Feshbach resonance delocalized scattering states acquire some bound-state character due to admixture of a bound level associated with a closed channel. It strongly enhances the Franck-Condon factor between the initial scattering state and a bound intermediate excited molecular state, a technique named Feshbach Optimized Photoassociation. We analyzed the transfer efficiency and intensities of the laser pulses required for optimal transfer both with and without the resonance and found that $> 70\%$ efficiencies are possible with relatively low intensity pulses of several W/cm^2 in the presence of the resonance.

5. Acknowledgments

We gratefully acknowledge finantial support from NSF and AFOSR under the MURI award FA9550-09-1-0588.

6. Appendix

A. Rotation and dephasing matrices

The Hamiltonian (2) in the case of the two-pulse STIRAP scheme, discussed in Section 2.1 has a zero eigenvalue $\varepsilon_0 = 0$, describing the dark state, and four eigenvalues, $\varepsilon_{1,2} = \pm\Omega\sqrt{1-\sin 2\theta/2}$ and $\varepsilon_{3,4} = \pm\Omega\sqrt{1+\sin 2\theta/2}$, corresponding to bright states. Adiabatic eigenstates $|\Phi\rangle = \{|\Phi^n\rangle\}$, $n = 0,...4$ and the bare states $|\Psi\rangle = \left\{\left|\Psi^l\right\rangle\right\}$, $l = g_1, e_1, g_2, e_2, g_3$ are transformed as $\left|\Psi^l\right\rangle = \sum_n W_{ln}\,|\Phi^n\rangle$, $|\Phi^n\rangle = \sum_l W_{ln}\left|\Psi^l\right\rangle$ via an orthogonal ($W^{-1} = W^T$) rotation matrix, given by the expression

$$W = \frac{1}{2}\begin{pmatrix} 2c^+c^- & s^- & s^- & s^+ & s^+ \\ 0 & 1 & -1 & -1 & 1 \\ 2s^-c^+ & -(s^- + c^-) & -(s^- + c^-) & (s^+ + c^+) & (s^+ + c^+) \\ 0 & -1 & 1 & -1 & 1 \\ -2s^+s^- & c^- & c^- & c^+ & (s^+ - c^+) \end{pmatrix},$$

where $c^{\pm} = \cos\theta/\sqrt{1 \pm \sin 2\theta/2}$, $s^{\pm} = \pm\sin\theta/\sqrt{1 \pm \sin 2\theta/2}$.
In the "straddling" STIRAP scheme the rotation matrix reads as:

$$W = \frac{1}{2}\begin{pmatrix} -2\cos\theta & 0 & \sin 2\theta\frac{\Omega}{\Omega_0} & 0 & -2\sin\theta \\ -\sqrt{2}\sin\theta & 2 & -\cos 2\theta\frac{\Omega}{\sqrt{2}\Omega_0} & -1 & \sqrt{2}\cos\theta \\ -\sqrt{2}\sin\theta & -1 & -\cos 2\theta\frac{\Omega}{\sqrt{2}\Omega_0} & 1 & \sqrt{2}\cos\theta \\ \sin\theta\frac{\Omega}{\Omega_0} & -1 & \sqrt{2} & -1 & \cos\theta\frac{\Omega}{\Omega_0} \\ \sin\theta\frac{\Omega}{\Omega_0} & 1 & \sqrt{2} & 1 & \cos\theta\frac{\Omega}{\Omega_0} \end{pmatrix},$$

where terms of the order of $O(\Omega^2/\Omega_0^2)$ and higher are neglected.
The Liouville operator in the bare state basis has a form

$$\mathcal{L}\rho = \frac{1}{2}\begin{pmatrix} 2\Gamma_1\rho_{g_1g_1} & (\gamma_1+\Gamma_1)\rho_{g_1e_1} & (\Gamma_2+\Gamma_1)\rho_{g_1g_2} & (\gamma_2+\Gamma_1)\rho_{g_1e_2} & \Gamma_1\rho_{g_1g_3} \\ (\gamma_1+\Gamma_1)\rho_{e_1g_1} & 2\gamma_1\rho_{e_1e_1} & (\gamma_1+\Gamma_2)\rho_{e_1g_2} & (\gamma_1+\gamma_2)\rho_{e_1e_2} & \gamma_1\rho_{e_1g_3} \\ (\Gamma_2+\Gamma_1)\rho_{g_2g_1} & (\gamma_1+\Gamma_2)\rho_{g_2e_1} & 2\Gamma_2\rho_{g_2g_2} & (\gamma_2+\Gamma_2)\rho_{g_2e_2} & \Gamma_2\rho_{g_2g_3} \\ (\gamma_2+\Gamma_1)\rho_{e_2g_1} & (\gamma_1+\gamma_2)\rho_{e_2e_1} & (\gamma_2+\Gamma_2)\rho_{e_2g_2} & 2\gamma_2\rho_{e_2e_2} & \gamma_2\rho_{e_2g_3} \\ \Gamma_1\rho_{g_3g_1} & \gamma_1\rho_{g_3e_1} & \Gamma_2\rho_{g_3g_2} & \gamma_2\rho_{g_3e_2} & 0 \end{pmatrix}.$$

We include the decay from the Feshbach and the intermediate state using a rate Γ_1 and Γ_2, respectively, and from the excited states $|e_{1,2}\rangle$, given by $\gamma_{1,2}$, and assume that all decay is due to population loss out of the system, e.g. to other vibrational levels or continuum. We also assume that molecules in the ground vibrational state $|g_1\rangle$ do not decay.

B. Adiabatic passage in the limits of broad and narrow Feshbach resonances

In this appendix, we discuss Eqs.(26) and (27) for various relative widths of the Feshbach resonance Γ with respect to the thermal energy spread δ_ϵ of the colliding atoms. We first describe the case of a broad resonance, *i.e.* when the width of the Feshbach resonance greatly exceeds the thermal energy spread ($\Gamma \gg \delta_\epsilon$), and second consider the opposite situation of a narrow resonance ($\Gamma \ll \delta_\epsilon$). Finally, we briefly present the case where there is no resonance.

B.1 Limit of a broad Feshbach resonance

The typical thermal energy spread for colliding atoms in photoassociation experiments with non-degenerate gases is $\delta_\epsilon \sim 10 - 100$ μK. The broad resonance case occurs for resonances having a width of several Gauss ($\sim$ 1 mK), for which we have $\Gamma/\delta_\epsilon \sim 10 - 100$. A wide variety of systems exhibit broad resonances. For instance, they can be found in collision of ^{6}Li atoms at 834 G for the $|f = 1/2, m_f = 1/2\rangle \otimes |f = 1/2, m_f = -1/2\rangle$ entrance channel (Γ = 302 G= 40 mK) and in ^{7}Li at 736 G for the $|f = 1, m_f = 1\rangle \otimes |f = 1, m_f = 1\rangle$ entrance channel (Γ = 145 G = 19 mK). We note here that these values of Γ are slightly different than the "magnetic" width ΔB usually given and based on the modelling of the scattering length.
The source function can be readily calculated from Eq.(31) by noticing that the Rabi frequency term can be set at $\epsilon = \epsilon_0$ corresponding to the maximum of the Gaussian function in the integrand. Using the function $g(q, \epsilon)$ defined in Eq.(32), the result takes the form

$$\begin{aligned} S_w &= S_0\sqrt{2\pi}\delta_\epsilon g(q,\epsilon_0)\mathrm{sgn}(\epsilon_0 - \epsilon_F)e^{-(t-t_0)^2\delta_\epsilon^2/2\hbar^2 - i(\epsilon_0/\hbar - (\omega_S - \omega_p))t} \\ &= S_{\mathrm{no-res}}g(q,\epsilon_0)\mathrm{sgn}(\epsilon_0 - \epsilon_F), \end{aligned} \tag{38}$$

where $S_{\mathrm{no-res}}$ is the source function without a resonance given below in Eq.(47). Strictly speaking, this expression is valid for $|\epsilon_F - \epsilon_0| \geq \delta_\epsilon$, but since $\Gamma \gg \delta_\epsilon$ Eq.(38) is a good approximation for a wide range of detunings $\epsilon_F - \epsilon_0$.
The back-stimulation term (34) can be further simplified in the limit of a broad resonance. In this case, both $c_2(t)$ and $\mathcal{E}_p(t)$ change on a time scale $\sim 1/\delta_\epsilon$, *i.e.* slowly compared to the decay time $\sim \hbar/\Gamma$ of the exponent. Therefore, we can rewrite (34) as:

$$\left|\frac{\vec{\mu}_{2\epsilon}\hat{e}_p}{\hbar}\right|^2 \pi\hbar \left[1 + \frac{(q-i)^2}{1 + 2i(\epsilon_F - \hbar(\omega_S - \omega_p))/\Gamma}\right] c_2(t)\mathcal{E}_p^2(t). \tag{39}$$

The system (26)-(27) in the case of a broad resonance becomes:

$$i\frac{\partial c_1}{\partial t} = -\Omega_S c_2, \tag{40}$$

$$i\frac{\partial c_2}{\partial t} = -\Omega_S c_1 - S_w + (\delta - i\gamma)c_2 - i\pi\hbar|\Omega_{\mathrm{no-res}}(t)|^2 \left[1 + \frac{(q-i)^2}{1 + 2i(\epsilon_F - \hbar(\omega_S - \omega_p))/\Gamma}\right] c_2, \tag{41}$$

where $\Omega_{\mathrm{no-res}} = \vec{\mu}_{2\epsilon}\hat{e}_p\mathcal{E}_p/\hbar$ is the continuum-bound Rabi frequency in the absence of resonance. We also added a spontaneous decay term γc_2, assuming that the excited molecules dissociate into high energy continuum states and the resulting atoms leave a trap. From Eq.(38), one can see that in a broad resonance case, the source amplitude is enhanced by the factor $g(q, \epsilon_0) = (q + 2(\epsilon_0 - \epsilon_F)/\Gamma)/\sqrt{1 + 4(\epsilon_0 - \epsilon_F)^2/\Gamma^2}$ when compared to the unperturbed continuum case. This factor has a maximum at $2(\epsilon_0 - \epsilon_F)/\Gamma = 1/q$, with the corresponding maximum value $g_{\max} \sim q$ for $q \gg 1$.

B.2 Limit of a narrow Feshbach resonance

This situation occurs when the width of the resonance is of the order of a few micro-Gauss or less. Examples of narrow resonances include ^{6}Li^{23}Na at 746 G for the $|f_1 = 1/2, m_{f1} = 1/2\rangle|f_2 = 1, m_{f2} = 1\rangle$ channel (Γ = 7.8 mG = 1 μK) (66), or ^{6}Li^{87}Rb at 882 G for the $|f_1 = 1/2, m_{f1} = 1/2\rangle|f_2 = 1, m_{f2} = 1\rangle$ channel (p-wave, Γ = 10 mG = 1.3 μK).
We note that the source term expressed in Eq.(31) can be rewritten in a time representation:

$$\begin{aligned} S = S_0\sqrt{2\pi}\delta_\epsilon e^{-i(\epsilon_0/\hbar - (\omega_S - \omega_p))t} \\ \times \left[e^{-(\tau-\tau_0)^2} + \xi e^{2iD - D^2}\int_{-\infty}^{\infty} e^{-(\tau' - iD)^2}(I_1(\xi|\tau - \tau_0 - \tau'|)\right. \\ -L_{-1}(\xi|\tau - \tau_0 - \tau'|) - iq(I_0(\xi|\tau - \tau_0 - \tau'|) \\ \left. -L_0(\xi|\tau - \tau_0 - \tau'|))\mathrm{sgn}(\tau - \tau_0 - \tau')d\tau'\right], \end{aligned} \tag{42}$$

where we introduced the dimensionless variables $\tau = t\delta_\epsilon/\sqrt{2}\hbar$, $D = (\epsilon_F - \epsilon_0)/\sqrt{2}\delta_\epsilon$, $\xi = \Gamma/\sqrt{2}\delta_\epsilon$; $I_{0,1}$ and $L_{0,-1}$ are modified Bessel and Struve functions. One can see from this expression that the source function is a sum of the pure source function of the unperturbed continuum, given by the first term in square brackets, and of the admixed bound state, given by the integral. The coefficient $\xi = \Gamma/\sqrt{2}\delta_\epsilon$, which is the ratio of the Feshbach resonance

width to the width of the thermal energy spread, gives the ratio of contributions from the bound state and the unperturbed continuum, respectively.
It is then easier to notice that in the limit of a narrow resonance, the Gaussian function in the integrand of Eq.(42) is much narrower than the Bessel and Struve functions, which change on the time scale $\sim 1/\xi$. Therefore the source term can be aproximated as:

$$\begin{aligned} S_n = S_0\sqrt{2\pi}\delta_\epsilon e^{-i(\epsilon_0/\hbar-(\omega_S-\omega_p))t}[e^{-(\tau-\tau_0)^2} \\ +\xi\sqrt{\pi}e^{2iD-D^2}(I_1(\xi|\tau-\tau_0|)-L_{-1}(\xi|\tau-\tau_0|) \\ -iq(I_0(\xi|\tau-\tau_0|)-L_0(\xi|\tau-\tau_0|))\mathrm{sgn}(\tau-\tau_0))]. \end{aligned} \tag{43}$$

Since $\xi \ll 1$, the real part of the source function is given by the first term in the square brackets, which is a pure continuum source function, while the imaginary part is due to the admixed bound state and its magnitude depends on the product ξq. Using asymptotic expansions of modified Bessel and Struve functions $I_0(x) - L_0(x) \to -2/\pi x$, $I_1(x) - L_{-1}(x) \to -2/\pi x^2$, it is seen from Eq.(43) that the contribution to the source function from the bound state decays on the time scale $|\tau - \tau_0| \sim 1/\xi$, while the contribution from the unperturbed continuum decays on the time scale $|\tau - \tau_0| \sim 1 \ll 1/\xi$.
In the limit of a narrow resonance the system (26)-(27) becomes:

$$i\frac{\partial c_1}{\partial t} = -\Omega_S c_2, \tag{44}$$

$$\begin{aligned} i\frac{\partial c_2}{\partial t} = -\Omega_S c_1 - S_n + (\delta - i\gamma)c_2 \\ -i\left|\frac{\vec{\mu}_{2\epsilon}\hat{e}_p}{\hbar}\right|^2\left[\pi\hbar\mathcal{E}_p^2 c_2 + \frac{\pi\Gamma}{2}(q-i)^2\mathcal{E}_p(t)\right. \\ \left.\times\int_0^t dt'\, c_2(t')\mathcal{E}_p(t')e^{\Gamma(t'-t)/2\hbar+i(\epsilon_F/\hbar-(\omega_S-\omega_p))(t'-t)}\right]. \end{aligned} \tag{45}$$

B.3 Continuum without resonance

Finally, let us consider the case of a continuum without resonance. In this case the continuum-bound Rabi frequency Eq.(29) is:

$$\Omega_\epsilon = \Omega_{\mathrm{no-res}} = \vec{\mu}_{2\epsilon}\cdot\hat{e}_p\,\mathcal{E}_p/\hbar, \tag{46}$$

and the source function is

$$S_{\mathrm{no-res}} = S_0\sqrt{2\pi}\delta_\epsilon e^{-(t-t_0)^2\delta_\epsilon^2/2\hbar^2-i(\epsilon_0/\hbar-(\omega_S-\omega_p))t}. \tag{47}$$

The back-stimulation term (34) reduces to

$$\left|\vec{\mu}_{2\epsilon}\cdot\hat{e}_p/\hbar\right|^2\pi\hbar\mathcal{E}_p^2 c_2 = \pi\hbar\left|\Omega_{\mathrm{no-res}}(t)\right|^2 c_2, \tag{48}$$

and the system (26)-(27) takes the simple form:

$$i\frac{\partial c_1}{\partial t} = -\Omega_S c_2, \tag{49}$$

$$i\frac{\partial c_2}{\partial t} = -\Omega_S c_1 + (\delta - i\gamma)c_2 - i\pi\hbar|\Omega_{\mathrm{no-res}}(t)|^2 c_2 - S_{\mathrm{no-res}}. \tag{50}$$

C. References

[1] D. DeMille, F. Bay, S. Bickman, D. Kawall, D. Krause Jr., S. E. Maxwell, L. R. Hunter, Phys. Rev. A 61, 052507 (2000).
[2] J. J. Hudson, B. E. Sauer, M. R. Tarbutt, E. A. Hinds, Phys. Rev. Lett. 89, 023003 (2002).
[3] D. W. Rein, J. Mol. Evol. 4, 15 (1974); V.S.Letohov, Phys. Lett. A 53, 275 (1975).
[4] V. V. Flambaum, M. G. Kozlov, Phys. Rev. Lett. 99, 150801 (2007).
[5] R. V. Krems, Int. Rev. Phys. Chem. 24, 99 (2005).
[6] M. A. Baranov, Phys. Rep. 464, 71 (2008).
[7] K. Goral, L. Santos, M. Lewenstein, Phys. Rev. Lett. 88, 170406 (2002).
[8] C. Trefzger, C. Menotti, B. Capogrosso-Sansone, M. Lewenstein, arxiv:1103.3145 (2011).
[9] D. DeMille, Phys. Rev. Lett. 88 067901 (2002).
[10] L. D. Carr, D. DeMille, R. V. Krems, J. Ye, New J. Phys. **11**, 055049 (2009).
[11] M. Lysebo, L. Veseth, Phys. Rev. A 83, 033407 (2011).
[12] A. Andre et al., Nat. Phys. **2**, 636 (2006).
[13] S. F. Yelin, K. Kirby, R. Côté, Phys. Rev. A **74**, 050301 (2006).
[14] T. Köhler, K. Góral, P. S. Julienne, Rev. Mod. Phys. 78, 1311 (2006).
[15] K. M. Jones, E. Tiesinga, P. D. Lett, P. S. Julienne, Rev. Mod. Phys. 78, 483 (2006).
[16] J. M. Sage, S. Sainis, T. Bergeman, D. DeMille, Phys. Rev. Lett. 94, 203001 (2005).
[17] A. Vardi, D. Abrashkevich, E. Frishman, M. Shapiro, J. Chem. Phys. 107, 6166 (1997).
[18] A. Pe'er, E. A. Shapiro, M. C. Stowe, M. Shapiro, J. Ye, Phys. Rev. Lett. 98, 113004 (2007); E. A. Shapiro, M. Shapiro, A. Pe'er, J. Ye, Phys. Rev. A 78, 029903 (2008).
[19] E. Juarros, P. Pellegrini, K. Kirby, R. Côté, Phys. Rev. A 73, 041403(R) (2006).
[20] M. Viteau, A. Chotia, M. Allegrini, N. Bouloufa, O. Dulieu, D. Comparat, P. Pillet, Science 321, 232 (2008).
[21] C. P. Koch, J. P. Palao, R. Kosloff, F. Masnou-Seeuws, Phys. Rev. A 70, 013402 (2004).
[22] V. N. Vitanov, M. Fleischhauer, B. W. Shore, K. Bergmann, Adv. At. Mol. Opt. Phys. 46, 55 (2001).
[23] K.-K. Ni, S. Ospelkaus, M. H. G. de Miranda, A. PeŠer, B. Neyenhuis, J. J. Zirbel, S. Kotochigova, P. S. Julienne, D. S. Jin, J. Ye, Science 322, 231 (2008).
[24] J. G. Danzl, M. J. Mark, E. Haller, M. Gustavsson, R. Hart, J. Aldegunde, J. M. Hutson, H. C. Nagerl, Nat. Phys. 6, 265 (2010).
[25] K. Winkler, F. Lang, G. Thalhammer, P. v. d. Straten, R. Grimm, J. H. Denschlag, Phys. Rev. Lett. 98, 043201 (2007).
[26] S. Ospelkaus, A. Pe'er, K. - K. Ni, J. J. Zirbel, B. Neyenhuis, S. Kotochigova, P. S. Julienne, J. Ye, D. S. Jin, arXiv: atom-ph: 0802.1093.
[27] E. A. Shapiro, M. Shapiro, A. Pe'er, J. Ye, Phys. Rev. A 75, 013405 (2007).
[28] W. C. Stwalley, Eur. Phys. J. D 31, 221 (2004).
[29] D. Jaksch, V. Venturi, J. I. Cirac, C. J. Williams, P. Zoller, Phys. Rev. Lett. 89, 040402 (2002).

[30] E. Kuznetsova, P. Pellegrini, R. Côté, M. D. Lukin, S. F. Yelin, Phys. Rev. A 78, 021402 (2008).
[31] B. W. Shore, K. Bergemann, J. Oreg, S. Rosenwaks, Phys. Rev. A 44, 7442 (1991).
[32] P. A. Ivanov, N. V. Vitanov, K. Bergmann, Phys. Rev. A 70, 063409 (2004).
[33] V. S. Malinovsky, D. J. Tannor, Phys. Rev. A 56, 4929 (1997).
[34] N. V. Vitanov, B. W. Shore, K. Bergemann, Eur. Phys. J. D 4, 15 (1998).
[35] S. T. Cundiff, J. Ye, Rev. Mod. Phys. 75, 325 (2003).
[36] D. S. Petrov, C. Salomon, G. V. Shlyapnikov, Phys. Rev. Lett. 93, 090404 (2004); D. S. Petrov, C. Salomon, G. V. Shlyapnikov, Phys. Rev. A 71, 012708 (2005).
[37] J. Cubizolles, T. Bourdel, S. J. J. M. F. Kokkelmans, G. V. Shlyapnikov, C. Salomon, Phys. Rev. Lett. 91, 240401 (2003).
[38] S. Jochim, M. Bartenstein, A. Altmeyer, G. Hendl, C. Chin, J. Hecher Denschlag, R. Grimm, Phys. Rev. Lett. 91, 240402 (2003).
[39] C. A. Regal, M. Greiner, D. S. Jin, Phys. Rev. Lett. 92, 083201 (2004).
[40] J. M. Hutson, P. Soldan, Int. Rev. Phys. Chem. 26, 1 (2007).
[41] T. Mukaiyama, J. R. Abo-Shaeer, K. Hu, J. K. Chin, W. Ketterly, Phys. Rev. Lett. 92, 180402 (2004).
[42] C. Chin, T. Kraemer, M. Mark, J. Herbig, P. Waldburger, H. - C. Hagerl, R. Grimm, Phys. Rev. Lett. 94, 123201 (2005).
[43] G. Smirne, R. M. Godun, D. Cassettari, V. Boyer, C. J. Foot, T. Volz, N. Syassen, S. Durr, G. Rempe, M. D. Lee, K. Goral, T. Köhler, Phys. Rev. A 75, 020702(R) (2007).
[44] J. J. Zirbel, K. - K. Ni, S. Ospelkaus, J. P. D'Incao, C. E. Wieman, J. Ye, D. S. Jin, arXiv: cond-mat: 0710.2479.
[45] A. Fioretti, C. Amiot, C. M. Dion, O. Dulieu, M. Mazzoni, G. Smirne, C. Gabbanini, Eur. Phys. J. D 15, 189 (2001).
[46] S. T. Thompson, E. Hodby, C. E. Williams, Phys. Rev. Lett. 95, 190404 (2005); T. M. Hanna, T. Köhler, K. Burnett, Phys. Rev. A 75, 013606 (2007).
[47] H. Y. Ling, H. Pu, B. Seaman, Phys. Rev. Lett. 93, 250403 (2004).
[48] E. Juarros, P. Pellegrini, K. Kirby, R. Cote, Phys. Rev. A 73, 041403(R) (2006).
[49] E. Kuznetsova, M. Gacesa, P. Pellegrini, S. F. Yelin, R. Côté, New J. Phys. 11, 055028 (2009).
[50] T. Mukaiyama, J. R. Abo-Shaeer, K. Xu, J. K. Chin, and W. Ketterle, Phys. Rev. Lett. 92, 180402 (2004).
[51] C. Chin, T. Kraemer, M. Mark, J. Herbig, P. Waldburger, H.-C. Nägerl, and R. Grimm, Phys. Rev. Lett. 94, 123201 (2005).
[52] A. Vardi, D. Abrashkevich, E. Frishman, M. Shapiro, J. Chem. Phys. 107, 6166 (1997).
[53] A. Vardi, M. Shapiro, K. Bergmann, Optics Express 4, 91 (1999).
[54] Ph. Courteille, R. S. Freeland, D. J. Heinzen, F. A. van Abeelen, B. J. Verhaar, Phys. Rev. Lett. 81, 69 (1998).
[55] F. A. van Abeelen, D. J. Heinzen, B. J. Verhaar, Phys. Rev. A 57, R4102 (1998).
[56] M. Junker, D. Dries, C. Welford, J. Hitchcock, Y. P. Chen, R. G. Hulet, Phys. Rev. Lett. 101, 060406 (2008).
[57] P. Pellegrini, M. Gacesa, R. Côté, Phys. Rev. Lett. 101, 053201 (2008).
[58] C. P. Koch and R. Moszyński, Phys. Rev. A 78, 043417 (2008).
[59] F. Lang, K. Winkler, C. Strauss, et al., Phys. Rev. Lett. 101, 133005 (2008);
[60] U. Fano, Phys. Rev. 124, 1866 (1961).

[61] M. Fleischhauer, A. Imamoglu, J.P. Marangos, Rev. Mod. Phys. 77, 633 (2005).
[62] A. C. Han, E. A. Shapiro, M. Shapiro, arxiv:1104.1480 (2011).
[63] C. Lee, E.A. Ostrovskaya, Phys. Rev. A 72, 062321 (2005).
[64] A. Griesmaier, J. Werner, S. Hensier, J. Stuhler, T. Pfau, Phys. Rev. Lett. 94, 160401 (2005).
[65] Z. Pavlovic, R. V. Krems, R. Côté, H. R. Sadeghpour, Phys. Rev. A 71, 061402 (2005).
[66] M. Gacesa, P. Pellegrini, R. Côté, Phys. Rev. A 78, 010701(R) (2008).

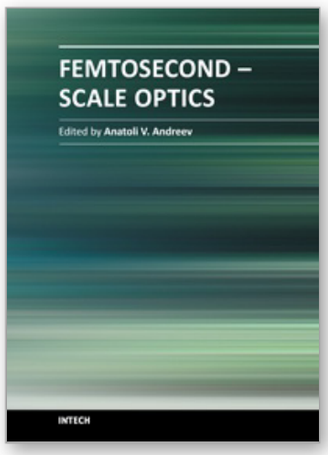

Femtosecond-Scale Optics
Edited by Prof. Anatoly Andreev

ISBN 978-953-307-769-7
Hard cover, 434 pages
Publisher InTech
Published online 14, November, 2011
Published in print edition November, 2011

With progress in ultrashort ultraintense laser technologies the peak power of a laser pulse increases year by year. These new instruments accessible to a large community of researchers revolutionized experiments in nonlinear optics because when laser pulse intensity exceeds or even approaches intra-atomic field strength the new physical picture of light-matter interaction appears. Laser radiation is efficiently transformed into fluxes of charged or neutral particles and the very wide band of electromagnetic emission (from THz up to x-rays) is observed. The traditional phenomena of nonlinear optics as harmonic generation, self-focusing, ionization, etc, demonstrate the drastically different dependency on the laser pulse intensity in contrast the well known rules. This field of researches is in rapid progress now. The presented papers provide a description of recent developments and original results obtained by authors in some specific areas of this very wide scientific field. We hope that the Volume will be of interest for those specialized in the subject of laser-matter interactions.

InTech Europe
University Campus STeP Ri
Slavka Krautzeka 83/A
51000 Rijeka, Croatia
Phone: +385 (51) 770 447
Fax: +385 (51) 686 166
www.intechopen.com

InTech China
Unit 405, Office Block, Hotel Equatorial Shanghai
No.65, Yan An Road (West), Shanghai, 200040, China
中国上海市延安西路65号上海国际贵都大饭店办公楼405单元
Phone: +86-21-62489820
Fax: +86-21-62489821

IntechOpen